

Modeling and Probing Strategy for Intelligent Transportation System Utilizing Lagrangian Traffic Data

by

Kang-Ching Chu

A dissertation submitted in partial fulfillment
of the requirements for the degree of
Doctor of Philosophy
(Mechanical Engineering)
in The University of Michigan
2016

Doctoral Committee:

Professor Kazuhiro Saitou, Chair
Research Assistant Professor Robert C. Hampshire
Assistant Professor Gábor Orosz
Professor Romech Saigal

© Kang-Ching Chu 2016
All Rights Reserved

To the memory of my beloved father,

Raymond T. Chu

(1932-2011)

who made me who I am today.

ACKNOWLEDGEMENTS

I would like to express my sincere gratitude to all the people who have made this dissertation possible. My deepest gratitude is to my research advisor, Dr. Kazuhiro Saitou, for his patient guidance, constant support, and kind encouragement. I am extremely lucky to meet Kazu who believed in me when I was frustrated and doubted myself after the first year of my doctoral study. He has been an incredible mentor who gave me the freedom to explore intellectually in my study, but at the same time provided the most inspired and valuable advice when I seek for help. What I learned from Kazu are not only approaches to conduct a quality research, but also his enthusiasm and attitude as a researcher. I would like to thank Dr. Romesh Saigal for sharing his knowledge with me and providing valuable advices to my study. He has been always patient to spend time and discuss questions in transportation that have deepened this research. I also want to thank Dr. Robert Hampshire and Dr. Gábor Orosz, who serve as my committee members, for offering their careful review and helpful suggestions to this dissertation.

I have been very lucky to meet and work with many intelligent graduate students, faculty members and researchers during the course of my study. I am especially grateful for the generous support and great work inspiration from Karim Hamza, Kazuhide Kaifuku, Jihun Kim, Jungkap Park, Yuqing Zhou and other previous and current members of Algorithmic Synthesis Laboratory in the Department of Mechanical Enigneering, and also Li Yang, Hao Zhou, Qi Luo, and Jiah Song from Dr. Saigal's research group in the Department of Industrial and Operations Engineering. I also

want to express my special thanks to Shuang Yin, who volunteered to help me process traffic data during the most critical time of finishing this dissertation.

I would also like to thank all the friends I met in Michigan. It has been a wonderful journey to be accompanied by their friendship, to encourage each other, and to enjoy all the laughs and tears together. Though I am thousands miles from home, they are my family here who helped me to adapt to a new environment, celebrated holidays together, and took care of me when I broke my right elbow one month before the completion of this dissertation.

Last, but not least, I would like to give my greatest thanks to my dearest family. My late father was the one who encouraged me to pursue my doctorate degree and made everything possible. Even though he did not get to see this dissertation completed, I know he would be happy and be proud of me. Thanks to my mother and my sister who always believe in me and allow me to go after my dream. This adventure of my graduate study would not be possible without their unconditional love, patience and support.

TABLE OF CONTENTS

DEDICATION	ii
ACKNOWLEDGEMENTS	iii
LIST OF FIGURES	vii
LIST OF TABLES	ix
ABSTRACT	x
CHAPTER	
I. Introduction	1
1.1 Motivation and Background	1
1.2 Dissertation Objective	3
1.3 Organization of the Dissertation	5
II. Related Work	7
2.1 Characteristics of Traffic State	7
2.2 Traffic Flow Model	9
2.3 Traffic Data Collection and Assimilation	12
2.4 Real-time Traffic State Estimation	15
2.5 Summary of Related Work	15
III. Eulerian Traffic Flow Modeling and Probe Vehicle Optimiza- tion	17
3.1 Overview	17
3.2 Macroscopic Traffic Flow Model	18
3.2.1 The LWR Model	18
3.2.2 The Speed-Density Relation	19
3.3 Newtonian Relaxation Method	20

3.4	Probe Vehicle Optimization Problem	21
3.4.1	Simulated Traffic Data	22
3.4.2	Probe Vehicle Deployment	23
3.5	Results	25
3.5.1	Single Objective: Density Estimation	27
3.5.2	Multi-objective: Estimation Error and Operation Cost	29
3.6	Conclusion	31
IV. Stochastic Lagrangian Traffic Flow Modeling and Real-time Traffic Prediction		34
4.1	Overview	34
4.2	Lagrangian Traffic Flow Model	35
4.3	Probing Method and Traffic Data	36
4.4	Real-time Traffic	37
4.4.1	Kalman Filter Method	38
4.4.2	Unscented Kalman Filter	39
4.4.3	State Space Models	41
4.4.4	Estimation of Current Traffic State and Traffic Prediction	42
4.5	Result from NGSIM Data	43
4.5.1	Traffic data and Traffic Phases on US-101	43
4.5.2	Real-Time Estimation of Current Traffic State	45
4.5.3	Prediction of Traffic State	46
4.5.4	Wide Moving Jam Detection	47
4.6	Result from Mobile Century Data	50
4.6.1	Traffic data and Traffic Phases on I-880	50
4.6.2	Estimation and Prediction of Traffic State with Scarce Probing Data	52
4.6.3	Wide Moving Jam Detection with Scarce Data	54
4.7	Adaptive Probing	54
4.8	Conclusions	59
V. Summary and Future Work		60
5.1	Dissertation Conclusion	60
5.2	Contribution	61
5.3	Future Work	62
BIBLIOGRAPHY		65

LIST OF FIGURES

Figure

1.1	Proposed model in an intelligent transportation system	4
2.1	Traffic phase definitions in Kerner’s theory: (a) Measured data of average vehicle speed in time and space. (b) Identified three phases on the time-space plane. (c) Time-dependences of speed at location 16.2 km . (d) Time-dependences of flow rate. (<i>Kerner et al. (2004a), Kerner (2009)</i>)	8
3.1	Probing data assimilation using nudging term	22
3.2	Illustration of the highway	23
3.3	Probe vehicle trajectories for baseline scenario	27
3.4	Fitness evolution of GA	28
3.5	Probe vehicle trajectories (GA)	28
3.6	Density result from GA	30
3.7	Pareto optimum result	31
3.8	Probe vehicle trajectories (MOGA)	31
3.9	Density result from MOGA	32
4.1	Probing vehicles in pair	38
4.2	Average speed in each cell on US-101	44
4.3	Observation of traffic state in each cell on US-101	45

4.4	Estimation of current traffic state in each cell on US-101	46
4.5	Absolute percentage error of 3-sec prediction in spacing on US-101 .	48
4.6	Observed right-hand-side of Lagrangian LWR model (ft/veh/sec) . .	49
4.7	Estimated α of current traffic state (ft/veh/sec)	49
4.8	Average speed in each cell on I-880	51
4.9	Estimation error in each cell on I-880	52
4.10	Loop detector location on I-880 (<i>Herrera et al. (2010)</i>)	53
4.11	Estimated cell size in each cell on I-880	54
4.12	Flow chart for adaptive probing	56
4.13	Mean absolute percentage error of adaptive probing	57
4.14	Data volume of adaptive probing	57
4.15	Data volume versus MAPE of adaptive probing	58

LIST OF TABLES

Table

3.1	Parameters used in the traffic data	24
3.2	GA and MOGA settings	26
4.1	Error of average spacing estimation of current traffic state on US-101	47
4.2	Error of 3-sec prediction of spacing on US-101	47
4.3	Error of average spacing estimation of current traffic state on I-880 .	51
4.4	Error of 9-sec prediction of spacing on I-880	55

ABSTRACT

Modeling and Probing Strategy for Intelligent Transportation System Utilizing
Lagrangian Traffic Data

by

Kang-Ching Chu

Chair: Kazuhiro Saitou

Traffic congestion in urban areas is posing many challenges, and traffic flow model that provides accurate traffic status estimation and prediction can be beneficial for traffic congestion management. Due to the limitation of the infrastructure, probing data from individual vehicles is an attractive alternative to inductive loop detectors as a mean to collect data for traffic information. In order to provide a better tool to monitor congestion and improve efficiency of the transportation system, the objective of this dissertation is to develop an analytical tool which predicts congested highway traffic by utilizing macroscopic traffic flow model and strategically collecting data from probing vehicles with real-time update. Macroscopic traffic flow models were used in the past to incorporate probe vehicle data and to provide real-time traffic information, but probing data collection has not been done strategically to match the need of the traffic flow model. Also, prediction of traffic state, especially for unexpected traffic jam, is needed to compensate latency in data processing and to provide advance warning to the driver.

First, based on the well-known Lighthill-Whitham-Richards (LWR) macroscopic traffic flow model, Newtonian relaxation method is used to incorporate probing data into the LWR model in Eulerian coordinates for traffic status estimation. An optimization scheme of probe vehicle deployment is used to investigate the trade-off between the quality of traffic flow estimation and operation cost. Synthetic data is used for numerical experiment, and Genetic algorithm is used to solve the optimization problem. The result indicates that optimal deployment of probe vehicle can reduce probing cost and estimation error by efficient usage of probe vehicles. It is possible to decrease probing data for congested traffic with negligible degradation on the quality of traffic status estimation.

Second, the LWR model is then converted into Lagrangian coordinates with a forcing function to form a stochastic Lagrangian macroscopic traffic flow model. Unscented Kalman filter is used to update the prediction of model parameters and traffic state in real-time. The proposed probing method tracks vehicles in pairs and utilizes loop detector data for additional information as needed. The model is validated with two sets of empirical data to demonstrate its capability of providing short-term prediction and using model parameter as a detector of traffic jam. Also, a scheme of adaptive probing is presented to show that adjusting probing cell size based on the variance from stochastic model can improve the prediction accuracy.

The traffic flow model proposed in this dissertation has the ability to accurately predict traffic state in real-time. An adaptive probing scheme based on prediction variance can efficiently use less data and provide higher information accuracy. Topics proposed for future research include the investigation of performance bounds, optimal sampling method for adaptive probing, investigation of traffic information distribution, and potential application of probing commercial vehicle with optimal operation.

CHAPTER I

Introduction

1.1 Motivation and Background

The performance of a transportation system is crucial to the economy and living quality of a community. The increasing traffic congestion level in the past decade has caused not only the problem of passenger delays but also a serious impact on vehicle emission pollution. A study of *FHWA* (2004) estimated that 32% of the daily travel in major US urban areas occurred under congested traffic condition. Also, in 2014, US drivers spent 6.9 billion hours of extra time sitting in the traffic burning 3.1 billion gallons of gas which caused a congestion cost of \$160 billion, according to the study of *Schrank et al.* (2015).

To cope with the problem, major efforts at reducing traffic congestion have been undertaken. Various forms of Intelligent Transportation Systems (ITS) that take real-time traffic data for decision support have been developed for this purpose. Real-time traveler information, adaptive ramp metering, and incident management are examples of such strategies, and real-time traveler information has been tested to have the greatest benefits among all single ITS strategies by *Chu et al.* (2004). Previous research of *Kang et al.* (2005) showed that the reduction of carbon-dioxide from transportation system can be achieved by providing traffic information. *Balakrishna et al.* (2005) showed that having partial vehicles with traffic information can benefit both

informed and uninformed drivers by improving utilization of the network capacity. Therefore, having a reliable and robust model to predict the traffic evolution and to provide traffic information is significant for controlling traffic congestion.

The success of using real-time traveler information at controlling congestion requires an model to accurately estimate the evolution of traffic flow, and a traffic flow model requires traffic data for calibration and continuous update. Therefore, data collection plays an important role in traffic condition estimation. In recent years, abundant traffic data has become available with the extensive use of detection and surveillance devices on the road. In many states of the United States, the administrators of the transportation departments have constructed databases that can provide historical and real-time traffic data to the public. Besides from traffic data collected from sensors installed at designated locations, it is also possible to collect trajectory data from vehicles traveling on the road. Vehicle-to-infrastructure (V2I) communication becomes more and more popular when GPS-enabled devices, such as smart phone and in-vehicle navigation device are widely available to the drivers. Some research institution conducted field experiments to record trajectory data from individual vehicles on the highway, such as the Next Generation Simulation (NGSIM) project of *US Department of Transportation* (2006) and the Mobile Century Experiment from *Herrera et al.* (2010). These datasets provide researchers an opportunity to develop traffic flow models with high volume of probe vehicle data.

Besides from the transportation authority and researchers who are interested in using traffic data for system level improvement in traffic congestion, individual drivers also benefit from the excessive amount of data available to the public and private traffic information providers. Social medial and map services such as Google Traffic, Waze, HERE Maps provide real-time traffic information to the users via smart phone and other wireless-enabled portable devices. Also, the development of autonomous vehicle requires more advanced and high definition map to make decisions in every

second in order to navigate through the traffic. Company like HERE, which provides HD map and traffic information to autonomous vehicle, has been working on a traffic probing system which turns individual phones into the resource of its real-time traffic information service. However, the so-called real-time traffic information is typically a few seconds delayed due to data processing and traffic estimation. Also, according to research conducted by *HERE* (2016), the accuracy of estimated time of arrival time estimation can increase by up to 20% with predictive traffic. While latency can be improved but not eliminated, even with few seconds of short-term traffic prediction can compensate for the delay and may improve the accuracy of traffic information.

Therefore, this research is motivated by the need of high quality traffic information for congested traffic management, and the potential of efficiently utilizing traffic data collecting from probe vehicles for traffic prediction using traffic flow model.

1.2 Dissertation Objective

In order to provide a better tool to monitor congestion and improve the efficiency of the transportation system, the objective of this research is to develop an analytical tool which predicts congested highway traffic by utilizing macroscopic traffic flow model and strategically collecting traffic data from probing vehicles with real-time updates. An overview of how the proposed model is used in an intelligent transportation system is illustrated in Figure 1.1. Traffic data assimilation includes collecting both probing data and fixed-location (loop detector) data. The collected data is fed into the macroscopic traffic flow model to perform real-time traffic prediction. The probing strategy is decided by the performance of traffic flow model and data availability to allow high quality traffic information to be provided to the drivers.

To achieve this objective, the following research questions will be addressed:

1. How to seamlessly incorporate probe vehicle data and loop detector data into a

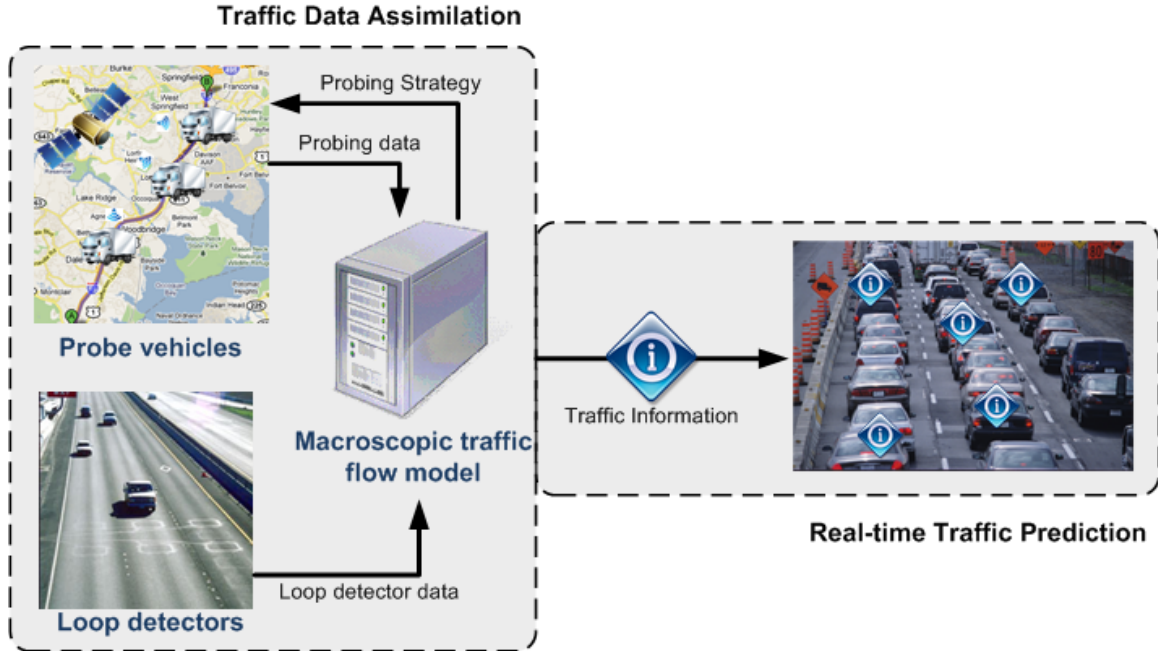


Figure 1.1: Proposed model in an intelligent transportation system

macroscopic traffic flow model to allow prediction of traffic status in real-time?

2. What is the probing strategy that allows high quality of traffic status prediction with low operation cost? What is the trade-off between cost and information quality?
3. How to detect congested traffic to compensate for the latency in real-time traffic information or even provide warning in advance?

In order to answer the first question, two different kinds of data assimilation method are used to incorporate probe vehicle data in macroscopic traffic models with different coordinate systems. First, Newtonian relaxation method is used to assimilate probing data into a deterministic traffic flow model in Eulerian coordinates. The second approach utilize a stochastic macroscopic traffic model in Lagrangian coordinates with Unscented Kalman filter to perform real-time traffic state prediction. The proposed Lagrangian model is validated using two different sets of empirical data

to show how to utilize evenly distributed probing data and a combination of scarce probing data and loop detector data.

For the second question, the optimization of probing vehicle deployment is first investigated by a multi-objective optimization problem which considers both operation cost of probing and the quality of traffic status estimation. Design variables are the probing timing and location. The numerical result using synthetic data from a simulated traffic reveals the benefit of optimal deployment and the trade-offs between cost and information quality. And then, in the Lagrangian coordinates, vehicles are probed in pairs to observe the change in spacing between vehicles. An adaptive probing scheme is proposed to adjust probing cell size based on the prediction variance from the stochastic model. Empirical data is used to demonstrate the benefit of using adaptive probing by comparing prediction error and required data volume.

For question 3, traffic state, including current and short-term prediction, can be estimated by the stochastic traffic flow model. Also, by developing the model with empirical data, the estimated model parameter in the traffic flow model is found to be useful in detecting traffic jam. Numerical result shows how the traffic flow model can provide advanced warning of unexpected traffic jam to the drivers.

1.3 Organization of the Dissertation

The rest of this dissertation is organized as follows:

Chapter II reviews related literature regarding background knowledge of traffic theory and traffic flow modeling, different types of traffic data and their utilization, and also previous work on real-time traffic estimation.

Chapter III presents the optimization for probing vehicle deployment when probing data is assimilated using Newtonian relaxation method with an Eulerian traffic flow model.

Chapter IV presents the proposed stochastic macroscopic traffic model in La-

grangian coordinates for real-time traffic prediction and the investigation of adaptive probing strategy.

Finally, Chapter V summarizes the presented work and the contribution of this dissertation. Future research topics and potential application of this work are also proposed in this chapter.

CHAPTER II

Related Work

2.1 Characteristics of Traffic State

An accurate traffic flow model is required to estimate and predict the evolution of traffic status, and it is particularly challenging to model congested traffic since the dynamic of congestion is more complex than free flow. Traditionally, free flow and congested flow are two traffic states which indicate traffic that allow vehicles to travel at speed limit and traffic that is under congestion, respectively. *Kerner* (2009) studied empirical data from freeways in Germany during 1995-2001 and proposed the three-phase traffic theory. He suggested that congested traffic should be further classified into two phases, the synchronized flow and the wide moving jam. The synchronized flow is a non-interrupted *flow* with its downstream front fixed at a bottleneck. The name *synchronized* comes from the tendency to a synchronization of speed across different lanes with low probability of passing. The other phase, the wide moving jam, is the stop-and-go phenomenon that travels backward in time and space domain and propagates through any other state of traffic flow and through any bottleneck. Traffic in the synchronized flow typically has decreased speed but remain moderate to high flow rate, but for the wide moving jam, low values in both speed and flow rate are observed in the traffic. Figure 2.1 shows the features mentioned above with measured traffic data. Though the three-phase theory was developed solely on

empirical observations of German freeways, traffic data from metropolitan areas in Germany, UK and the US all showed promising results in observing all three traffic phases which reflects Kerner's theory as discussed in *Rehborn et al.* (2011).

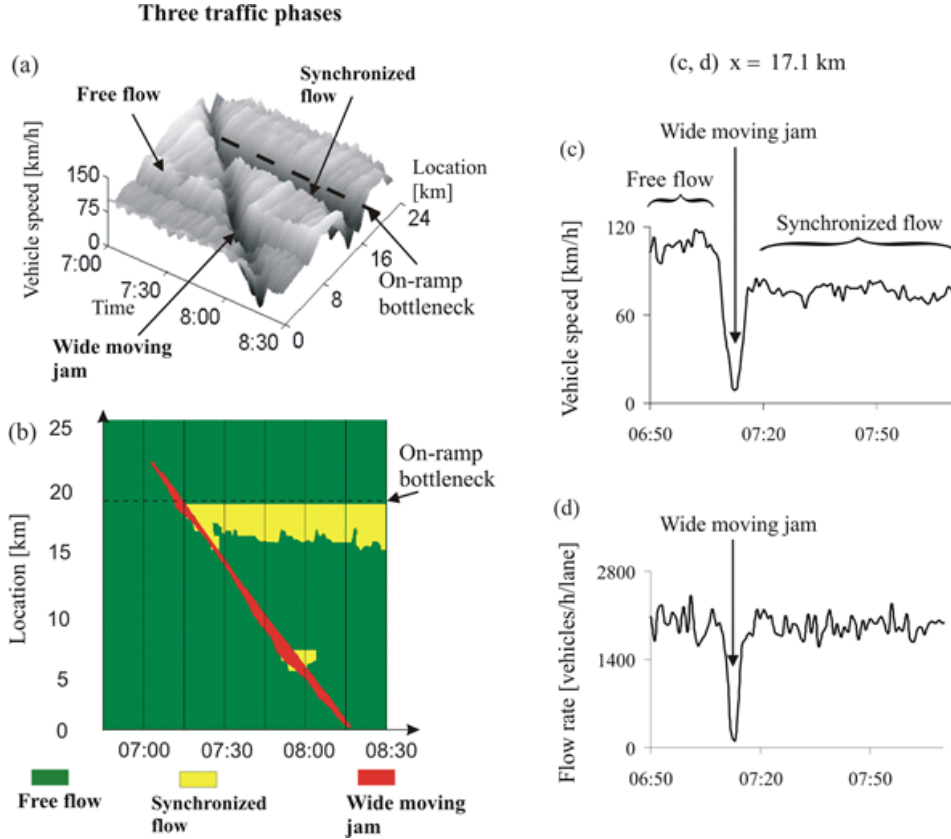


Figure 2.1: Traffic phase definitions in Kerner's theory: (a) Measured data of average vehicle speed in time and space. (b) Identified three phases on the time-space plane. (c) Time-dependences of speed at location 16.2 km . (d) Time-dependences of flow rate. (*Kerner et al.* (2004a), *Kerner* (2009))

Among the three traffic phases, the unexpected characteristic of the wide moving jam makes it more difficult to predict or to provide advanced warning to the drivers. Methods to detect transitions between any two traffic phases was investigated through the use of loop detectors data by *Kerner* (2009) and probing data from individual vehicles by *Kerner et al.* (2013). The detection of transitions relies on using speed and flow rate data collected by loop detectors on the road, or sensing probing vehicles traveling at a threshold speed taking longer than a threshold time. Boundaries

of traffic phase are then constructed after the identification of the transition points. However, the critical speed, critical flow rate, and time thresholds depend on a particular road stretch and have to be pre-determined by analyzing historical traffic data. The FOTO (Forecasting of Traffic Objects) and ASDA (Automatische Staudynamik-analyse: Automatic Tracking of Moving Jams) models (*Kerner et al. (2004b)*) were developed to reconstruct and track the synchronized flow and the wide moving jams, respectively. Unlike traffic flow model approaches in the next section which are based on flow dynamics, ASDA/FOTO models are based on spatiotemporal features of traffic congestion observed in measured traffic data from road detectors (*Kerner et al. (2004a)*) and probe vehicles (*Rehborn et al. (2012)*). The models predict the propagation of synchronized flow and wide moving jam after the two phases are initially identified with the measured data, and then the models use cumulative flow approach and Stokes shockwave formula to track the downstream and upstream fronts of the synchronized flow and the wide moving jam.

2.2 Traffic Flow Model

Other than data-driven traffic flow theory, macroscopic and microscopic are two main mathematical approaches to model the traffic. Microscopic approaches see traffic in the view of movements of individual vehicles. The model captures the interaction among vehicles, and may also consider interaction between the driver and the vehicle. One example of the microscopic traffic model is the car-following model, which considers how the drive follows its leading vehicle in the traffic to make decision on vehicle speed, acceleration, and distance to the leading vehicle. *Pipes (1953)* developed the first car-following model based on the assumption that the driver would keep a safe distance, which is related to the speed. While car-following model is used for single lane, situation include multiple lanes would require a model such as Gipps model (*Gipps (1986)*) to consider the lane change behavior. A combination

of microscopic behavior models, includes car-following, lane-changing, and other individual driver behavior models can be used to construct a simulation to investigate multi-lane traffic flow dynamics as shown by *Hodas and Jagota (2003)*. Many well-developed microscopic traffic simulation tools are available for research and design of transportation system, such as Aimsun (*TSS-Transport Simulation Systems (2010)*), MITSimLab (*MIT Intelligent Transportation Systems Program (2010)*), PARAMICS (*Quadstone Paramics Ltd (2011)*), VISSIM (*PTV Planung Transport Verkehr AG (2011)*), and POLARIS(*Auld et al. (2015)*). Microscopic simulation tools have been used for wide range applications in network design, analysis of transportation problems, and the evaluation of ITS and traffic management strategies. One benefit of having simulation model is that it provides traffic information at both transportation system level and individual vehicle level, so it can be used to experiment traffic management strategy and to evaluate its impact to the entire network and individuals. Microscopic traffic simulation with appropriate assumption and calibration can be used to validate traffic congestion model (*Kurihara et al. (2009)*) and to observe macroscopic phenomena in order to understand the influence of individual driver's behavior (*Goldbach et al. (2000)*). *Chu et al. (2011)* used real traffic data and microscopic simulation model to reconstruct highway traffic as a platform to validate a stochastic macroscopic traffic flow model. However, when microscopic simulation can be considered as an alternative of field experiment and empirical data, it requires a lot of effort to tune the parameters in the simulation in order to represent the actual traffic.

Macroscopic traffic flow models, which assume that traffic flow is comparable to fluid flow, have the advantage for real-time applications because of the lower computational cost and the relatively simple calibration comparing to microscopic simulation models. The simple yet insightful Lighthill-Whitham-Richards (LWR) model (*Lighthill and Whitham (1955)*; *Richards (1956)*) based on fluid dynamics has been

widely studied since its first appearance in 1955. It treats traffic flow as a compressible fluid and studies properties induced by the interaction of a group of vehicles while ignoring the details and identities of individual vehicles. While the original LWR model is a continuous macroscopic model, *Daganzo* (1994) proposed a discretized version of LWR model, which is known as *cell transmission model* (CTM). CTM uses Godunov Scheme (*Godunov* (1959)) to simulate macroscopic traffic flow evolution when dividing a given stretch into homogeneous sections (*Lebacque* (1996)). Although the LWR model fails to explain several minor phenomena, including hysteresis and traffic oscillations (*Li et al.* (2012)), its hydrodynamic approach that implements mass conservation in traffic flow is valid for homogeneous traffic flow.

While most research on the LWR model are in the traditional Eulerian coordinates, there are some efforts on modeling traffic flow in Lagrangian coordinates. Instead of the Eulerian coordinate system in time and space, the Lagrangian LWR model uses the coordinate system time and cumulative count to follow the vehicle trajectory. The use of cumulative flow as for traffic flow modeling is first proposed by *Newell* (1993) based on the conservation law in Lagrangian coordinates from gas dynamics (*Courant and Friedrichs* (1999)), and Newell's solution is then proved by *Daganzo* (2005) using variation theory. *Leclercq et al.* (2007) proposed the usage use cumulative flow as the Lagrangian coordinates of traffic flow model and discussed the benefit of using Lagrangian approach in theory. Using LWR model in Lagrangian coordinates with empirical data validation was then investigated by *Yuan et al.* (2012) and *Van Wageningen-Kessels et al.* (2013).

Other efforts have been done to improve LWR model, such as including higher order terms, adding sink and source terms to flow conservation, or considering stochastic nature of the traffic. Some of the widely accepted higher order models include momentum equation on top of the mass conservation of LWR model. Payne-Whitham (PW) model (*Payne* (1971), *Whitham* (1974)) was the first approach to add another

partial differential equation to emulate the momentum equation from fluid flow. Aw-Rascle model (*Aw and Rascle (2000)*) modified the space derivative of pressure in the momentum equation of PW model to correct the issue of second-order model criticized by *Daganzo (1995)*. Zhang’s model (*Zhang (2002)*) included the momentum equation which is derived from a microscopic car-following model. There are other modifications of LWR model, for example, *Papageorgiou et al. (1990)* and *Yuan et al. (2012)* added extra functions to consider on and off ramp flow, which also result in more parameters for calibration.

Due to the stochastic nature and uncertainty of the traffic, some work introduced stochasticity to the traffic flow model. *Boel and Mihaylova (2006)* proposed a compositional stochastic model based on CTM model by introducing random variables to sending and receiving functions. *Saigal et al. (2011)* proposed a stochastic partial differential equation (SPDE) model with a forcing function to the mass conservation in the LWR model for traffic flow prediction. The forcing function captures the variation of congestion with space and time and gradually reverts to the mean values after any random perturbations. While stochastic models can perform better than deterministic model by comparing mean output of stochastic model, the variance of stochastic model which can be interpreted as the confidence level of the prediction is usually missing from the discussion. *Jones et al. (1998)* discussed the benefit of having a combination of low- and high-fidelity sampling scheme when using a stochastic process approach to approximate function in global optimization. The variance from stochastic traffic flow model may be utilized in a similar manner to adjust probing samples to perform traffic estimation.

2.3 Traffic Data Collection and Assimilation

Fixed-location inductive loop detectors are the most common source of traffic data, which are sensors installed in the pavement to collect information such as vehi-

cle count, speed and occupancy. Traffic data from inductive loop detectors is collected with a constant time interval, usually 30 to 60 seconds. This type of data, distributed evenly in time and space, are known as Eulerian data. It can be easily used in the macroscopic traffic model for traffic status estimation, since traffic model is usually discretized in time and space. However, the high installation cost, difficulty of maintenance and lack of flexibility after installation are some of the disadvantages of employing loop detectors. Traffic model development has suffered from limited availability and quality of loop detector data for model calibration and validation. On the other hand, collecting traffic data using individual vehicle equipped with Global Positioning System (GPS), also known as probe vehicle, can be another way to monitor the traffic. Because of the decreasing cost and increasing accuracy of GPS technology, devices such as automotive navigation systems and GPS-enabled cell phones are becoming more and more common in the market. Therefore, probing data has been an interest of researchers for the benefit of flexibility and quick deployment.

Previous work using field experiment data found the benefit of having probing data or a mixture of probing and loop detector data. One early usage of probe vehicle is *Barth et al.* (1996). A field experiment on a freeway in San Diego, California was conducted to obtain traffic data from fixed sensors and a single probe vehicle to reveal the benefit of using probing data for microscopic and macroscopic traffic information. *Barth and Boriboonsomsin* (2009) also use sensors and multiple probing vehicles in the traffic to demonstrate how traffic information can be used to save 10-20 % of fuel consumption in the transportation system. Including probing data can improve the accuracy of travel time estimation up to 50% when loop detectors are spaced more than 2.11 miles apart, according to the simulation result from *Mazaré and Tossavainen* (2012). Also, while the research of *Rehborn et al.* (2012) used probing data only for traffic congestion warning, it showed that probe vehicles with a penetration of around 2% of the total traffic flow would be good enough to identify

traffic jam pattern in the traffic. However, in reality, it is a challenge to maintain sufficient penetration of probe vehicle for the purpose of traffic modeling. Research from BMW Group (*Breitenberger et al. (2004)*) concluded that a penetration rate of 7-10% would be required throughout Germany for high information quality in urban areas and on Federal roads, and off-peak hours require almost doubled probe vehicle penetration rate compared to peak hours.

Traffic data collection has changed dramatically with the availability of big data collected from probe vehicles, and data screening and processing become crucial for real-time update of traffic information. While conventional traffic flow models are formulated in Eulerian coordinate system, probing data which follows the trajectory of each probe vehicle is known as Lagrangian data. Lagrangian data would require certain processing to be incorporated into traffic flow model in Eulerian coordinates in order to estimate traffic status at each time and location. *Work et al. (2010)* introduced Virtual Trip Lines (VTLs), which can be understood as virtual loop detector on the road. Position and speed data is recorded when probe vehicles passes each VTL to allow the LWR model in Eulerian coordinates to estimate average travel speed in real-time with Ensemble Kalman filter (EnKF). *Herrera and Bayen (2010)* used Newtonian relaxation (or nudging) method from oceanography and Kalman Filter method to incorporate Lagrangian data for traffic status estimation. Another approach is to consider using Lagrangian flow model. *Yuan et al. (2012)* shown that using LWR model in Lagrangian coordinates with Lagrangian sensor data provides improvement in accuracy and offers computational benefits over the Eulerian approach for real-time applications. However, since the penetration rate of probing would significantly affect the performance of traffic status estimation, Lagrangian flow model may still need to account for loop detector data as needed.

2.4 Real-time Traffic State Estimation

As mentioned earlier, real-time application is one of the advantage of macroscopic traffic flow model, and Kalman filter is an effective method for recursive traffic status estimation in real-time. Due to the nonlinear state transition in the traffic flow model, various forms of nonlinear Kalman filter was used with success. Extended Kalman filter (EKF) was used in the past for its advantage in low computational cost. *Wang and Papageorgiou (2005)* used a second-order stochastic macroscopic model and applied EKF to estimate traffic density, speed, and model parameters simultaneously. The model was later validated with loop detector data from a highway stretch in Germany (*Wang et al. (2007)*). *Yuan et al. (2012)* also used EKF to perform real-time traffic estimation with a Lagrangian LWR model. However, the linearization in EKF could be difficult for highly complex nonlinear system. On the other hand, unscented Kalman filter (UKF) proposed by *Julier and Uhlmann (2004)* uses a mathematical sampling technique called unscented transform to estimate the mean and covariance of the output variable from a nonlinear transformation of the input variable. UKF is expected to provide better approximation while the state transition is highly nonlinear. By using simulation to compare EKF and UKF, *Hegyi et al. (2006)* claimed that the performance of both method is comparable, even though UKF propagates the state noise distribution better. *Mihaylova et al. (2007)* and (*Yang (2012)*) compared UKF and Particle filter (PF), also know as Sequential Monte Carlo (SMC) for traffic status estimation. Their results showed that PF could have equal or better performance than UKF, but PF is much more computationally expensive.

2.5 Summary of Related Work

This chapter provides a comprehensive review of related literature. Kerner's three-phase traffic theory provides the insight of congested traffic and reveals different

characteristics of the synchronized flow and the wide moving jam. Tools have been developed to use spatiotemporal features of traffic and to track the propagation of the synchronized flow and the wide moving jam. The development of macroscopic traffic flow modeling shows the benefit of using simple LWR model with some modification to account for inflow, outflow and random behavior on the highway. Stochastic models have been implemented to capture the randomness in the traffic with better prediction capability. While probing vehicle data is a popular resource of traffic data, there are some but limited efforts on incorporating LWR model with Lagrangian data or using Lagrangian model. Kalman filter method is commonly used to recursively update traffic information in real-time, and method like UKF is capable for nonlinear state transition in the traffic flow model.

This dissertation would focused on some of the issues and questions that are still unsolved by the previous work. First, while prediction of traffic state, especially for the unexpected wide moving jam, is needed to compensate latency in data processing and to provide advance warning to the driver, it is not demonstrated if macroscopic traffic flow model is capable of capturing congested traffic in both the synchronized flow and the wide moving jam phases. Second, previous work utilize probing data are usually done by using all the available data or random samples. However, the requirement of data can be varied by traffic condition, and probing may be optimized and adaptively decided. Also, while the distribution of traffic state prediction from stochastic model reveals the confidence level of mean output, previous work ignored the variance and used only the mean output to compare its performance to the deterministic model. It is remain unexplored if the output prediction variance of the stochastic model can be used to dynamically adjust input probing data for adaptive probing.

CHAPTER III

Eulerian Traffic Flow Modeling and Probe Vehicle Optimization

3.1 Overview

When the traffic management agency oversees the transportation network, the usage of the Eulerian coordinates is preferable to locate congested areas and to apply regional traffic control strategies. The Eulerian LWR model is used as the fundamental of the traffic status estimation, and a data assimilation technique, Newtonian relaxation method, has been successfully used to incorporate probe data into the macroscopic traffic flow model (*Herrera and Bayen (2010)*). However, previous work only used probe data passively as a data resource by utilizing all the possible probing data without considering the efficiency and the cost of probing. The study of *Breitenberger et al. (2004)* indicated that different probing data may be required under different traffic condition. Therefore, this chapter would focus on developing the optimal strategy for probe vehicle deployment and data collection. The optimization would consider both the operation cost of probing and the performance of traffic status estimation using the Eulerian traffic flow model. Synthetic traffic is used in the optimization problem to show numeral result. The trade-off between the quality of traffic density estimation and operation cost of probing are investigated using

multi-objective genetic algorithm.

3.2 Macroscopic Traffic Flow Model

Since its proposal in 1950s, the classical LWR model has been the building block of many macroscopic traffic flow models. It is a partial differential equation, and three primary aggregated variables, flow rate, density, and average speed, are used to describe the traffic in a macroscopic traffic flow model. The notation is described as below:

- (x, t) is the Eulerian coordinates with location and time, $x \in [0, L]$ and $t \in [0, T]$;
- $Q(x, t)$ is the flow rate (i.e, number of vehicles passing through per unit time) at location x and time t ;
- $\rho(x, t)$ is the density (i.e, number of vehicles per unit distance) at location x and time t ;
- $v(x, t)$ is the average velocity of all vehicles at location x and time t .

For simplicity, Q, ρ, v may be used in subsequent discussion with the understanding that these quantities are dependent on x and t .

3.2.1 The LWR Model

The LWR model is presented in Equation (3.1) and Equation (3.2). The first one is a first-order partial differential equation derived from the conservation law, which can be understood as that the difference of the inflow and the outflow in a cell is equal to the increment of the vehicles in the cell. The second equation is called fundamental flow relationship. It reflects the relationship among Q , ρ and v , since they are not independent.

$$\frac{\partial}{\partial t}\rho + \frac{\partial}{\partial x}Q = 0 \quad (3.1)$$

$$Q = \rho \cdot v \quad (3.2)$$

The LWR model assumes that the traffic flow reaches the equilibrium state immediately. It performs well for modeling heavy traffic on the highway when drivers can not do much but following the flow. Critics of LWR model include that it fails to capture the traffic under low density, assumes no on-ramp and off-ramp, and ignores the stochastic nature of the traffic. A stochastic partial differential equation (SPDE) model building on the classic LWR traffic flow model was then developed by *Saigal et al.* (2011) to improve the original LWR model. The SPDE model includes a forcing term to Equation (3.1) in order to capture the variation of congestion in space and time and gradually revert density to its mean value after an random perturbation. The validation using microscopic traffic simulation suggests that the SPDE model is capable of capturing some of the stochastic nature of the traffic flow evolution and improving the accuracy of prediction (*Chu et al.* (2011)). This SPDE model will be used to generate simulated traffic data for this work, and the detail will be described in section 3.4.1.

3.2.2 The Speed-Density Relation

As shown in equation (3.2), given any two of Q , ρ , and v , the remaining third can be determined. If the speed-density function, $v(\rho)$, is known, the traffic flow model is determined only by the functional ρ . The relationship between flow rate and density is usually called the *Fundamental Diagram* of traffic flow, which may also be written in the form of speed and density relation using Equation 3.2. The fundamental diagram provides the relation between speed and density base on the

phenomenon that greater number of vehicles on a road would result in slower speed. Several functional forms of the speed and density relation have been proposed in the past, they usually include constants, such as free-flow speed v_f and critical density ρ_j , in the function. Some of them have been frequently used in the literature, for example, *Greenshields et al.* (1935) considered a linear relationship as $v_f(1 - \rho/\rho_j)$, *Greenberg* (1959) proposed a logarithmic relationship as $v_0 \ln(\rho_j/\rho)$, and *Underwood* (1961) used exponential form, $v_f \exp(-\rho/\rho_j)$. Since some speed-density functions are more appropriate for congested traffic while others are more suitable for free flow, it is possible to mix them in application by adopting one in congested space-time sections and another for the free-flow sections. However, it requires data fitting with the field data to decide a better functional form, and the result may vary from field data of different dates/times and locations. We adopt the log piecewise linear model in Equation (3.3) as the speed-density function in this study, which has been examined to have the best fit using traffic data from highway I-95 in Virginia by *Saigal et al.* (2011).

$$v = \min\{v_f, \alpha\rho^m\} \tag{3.3}$$

where α and m are constants which can be calibrated by the field traffic data.

3.3 Newtonian Relaxation Method

The Newtonian relaxation method was originally formulated to estimate the velocity field of rivers using GPS-equipped drifters, which is analogous to having probe vehicles for traffic status estimation as used in *Herrera and Bayen* (2010). It adds a nudging term into the right hand side of Equation (3.1) to relax the dynamic model of the system towards the observations. For each probe vehicle k , it observed position $s_k^o(t_k^p)$ and velocity $v_k^o(t_k^p)$ at past time t_k^p , and then density can be derived from speed-

density function as $\rho^o(s_k^o(t_k^p), t_k^p)$. The estimated density $\hat{\rho}$ at time t and location x can be presented in the form of LWR model using probe data from a total number of K probe vehicles as in Equation (3.4).

$$\frac{\partial \hat{\rho}}{\partial t} + \frac{\partial q(\hat{\rho})}{\partial x} = - \sum_{k=1}^K \sum_{t_k^p \in \Omega_k^t} \lambda(x - s_k(t_k^p), t - t_k^p) \cdot [\hat{\rho}(s_k(t_k^p), t_k^p) - \rho^o((s_k(t_k^p), t_k^p))] \quad (3.4)$$

Note that Ω_k^t is the set of past times until t when vehicle k has observation recorded, and t_k^p should be smaller than t . The nudging term is proportional to the difference between estimated density and observation, and then a nudging factor λ is used to weight each observation. The nudging factor presented in Equation (3.5) depends on how far away (δ_x) and how long ago (δ_t) the observation is measured. Parameters X_{nudge} and T_d decided the range of observation to be included in space and time, respectively, and T_a determines the strength of the nudging factor. The usage of nudging term and nudging factor is illustrated in Figure 3.1.

$$\lambda(\delta_x, \delta_t) = \begin{cases} \frac{1}{T_a} \exp\left(-\left(\frac{\delta_x}{X_{nudge}}\right)^2\right) \exp\left(-\frac{\delta_t}{T_d}\right), \\ \text{if } |\delta_x| \leq X_{nudge} \text{ and } 0 < \delta_t \leq T_d \\ 0, \text{ otherwise} \end{cases} \quad (3.5)$$

3.4 Probe Vehicle Optimization Problem

In order to investigate how the deployment of probe vehicle would influence the traffic status estimation, traffic data is required for testing and demonstration. The hypothetical test traffic is generated via a simulation which is based on the SPDE model, and this synthetic traffic is used in the proposed scenario of probe vehicle deployment problem. This section would explain the simulated traffic and the setting

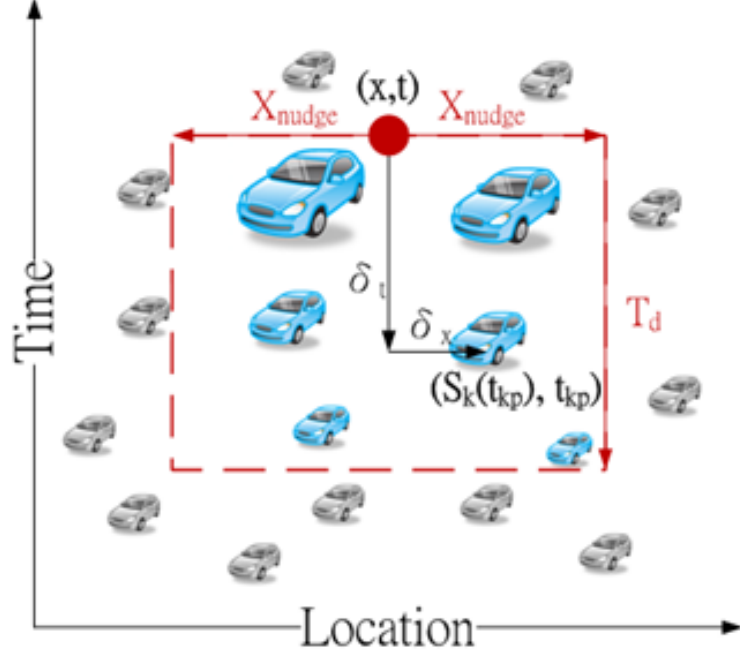


Figure 3.1: Probing data assimilation using nudging term

of the optimization problem.

3.4.1 Simulated Traffic Data

Synthetic traffic data is generated through a simulation with traffic on a 12-mile highway stretch which is equally divided into 20 cells with the length of 0.6 miles per cell. The SPDE model used to run the simulation is presented as follow:

$$\begin{aligned} \frac{\partial}{\partial t}\rho(x, t) + \frac{\partial}{\partial x}Q(\rho(x, t)) &= g(\rho(x, t), x, t), \\ g(\rho, x, t) &= a(x, t) + b(x, t) \cdot \rho + \sigma(x, t) \cdot W(dx, dt). \end{aligned}$$

A forcing term $g(\rho(x, t), x, t)$, composed of three deterministic parameters $a(x, t)$, $b(x, t)$, $\sigma(x, t)$, and a Brownian Sheet W (*Walsh* (1986)), is added to the classic LWR model on traffic density. The parameter $a(x, t)$ is the drift term designed to capture the effects of the entering flow from the entrance ramp. The traffic leaving

the highway through the exit ramp is assumed to be proportional to the traffic density near the exit ramp and $b(x, t) \cdot \rho$ represents the leaving traffic. The function $\sigma(x, t)$ is designed to capture the magnitude of the disturbance to the flow conservation due to the microscopic effects along the highway when the Brownian sheet W is a Gaussian process indexed by two parameters x and t with $E[dW(x, t)] = 0$ and $Var[dW(x, t)] = dx \cdot dt$.

In the simulation, the forcing function parameters $a(x, t)$, $b(x, t)$, and $\sigma(x, t)$ are assigned to represent traffic evolution from free flow to congestion, and then return to free flow in a 3-hour simulation run. More vehicles are staying on the highway after the first 30 minutes of the simulation, and this would cause a congestion in the following 1.5 hours. Traffic density is collected every minute in each cell to generate ground truth density. Six loop detectors are placed on the highway at cell 3, 6, 9, 12, 15, and 18, which measure the ground truth density every minute. Probe vehicles observe speed every minute with a measurement noise ϵ^v , and then the speed-density relationship is used to get observed density from speed measurement. The probing data collected by each vehicle includes time, location, speed and density. Figure 3.2 presents the highway stretch and illustrates the loops detectors as triangles. The parameters used for speed-density relationship and the measurement error are concluded in Table 3.1

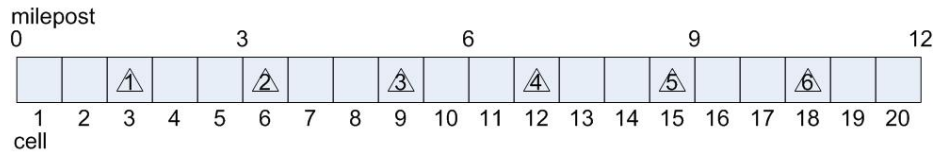


Figure 3.2: Illustration of the highway

3.4.2 Probe Vehicle Deployment

Assuming a fixed number of K probe vehicles available, the design variables are the original o_k and destination d_k of each vehicle k and departure time OT_k . Because

Table 3.1: Parameters used in the traffic data

Parameters	Values	Descriptions
v_f	65 miles/hr	Free flow speed
m	-1.2	Speed-density function parameter
α	9000 vehicle/hr	Speed-density function parameter
$Var[\epsilon^v]$	4^2 (miles/hr) ²	Variance of speed measurement noise, $\mu[\epsilon^v] = 0$

vehicles have to follow the traffic after departure, the location of the vehicle at any time t_k^p is $s_k(t_k^p)$ and can be calculated as follow:

$$s_k(t_k^p) = \int_{OT_k}^{t_k^p} v(s_k(\delta), \delta) d\delta + o_k \quad (3.6)$$

The location of o_k and d_k would be converted from milepost into corresponding cell index as O_k and D_k . Consider that the original/destination locations and time are where and when the probing occurs on a vehicle, O_k and D_k do not need to be constrained by the on- and off-ramp of the highway. Therefore, O_k and D_k are only constrained to be between the interested highway stretch from cell 1 to N .

$$1 \leq O_k \leq N, k = 1, \dots, K \quad (3.7)$$

$$1 \leq D_k \leq N, k = 1, \dots, K \quad (3.8)$$

In order to ensure proper probing data collection, D_k is set to be at least two cells from O_k .

$$O_k - D_k \leq -2, k = 1, \dots, K \quad (3.9)$$

The traffic status estimation is performed by obtaining density at each (x, t) using Equation (3.4) with data from probe vehicles only. The estimated density would be

compared to the ground truth density measured by each loop detector l located at x_l to evaluate the performance. So the first objective function is the overall root mean square error (RMSE) across all the loop detectors:

$$\text{RMSE} = \sqrt{\frac{\sum_{l \in M} (\hat{\rho} - \rho(x_l, t))^2}{n}} \quad (3.10)$$

where M is the set of all the loop detectors, and density from loop detector l at time t is $\rho(x_l, t)$ with a total of n observations.

Another objective considered is the operation cost of probing. Assuming the cost is proportional to the duration of probing, and the rate is C , then the cost can be represented as:

$$\text{cost} = C \sum_{k=1}^K (DT_k - OT_k) \quad (3.11)$$

where DT_k is the destination time, which is recorded in the probe data.

With the design variables, constraints, and objectives described above, the optimization problem can be formulated as the follows:

$$\begin{aligned} & \text{minimize } \{\text{RMSE}, \text{cost}\} \\ & \text{subject to } 1 \leq O_k \leq N, k = 1, \dots, K \\ & \quad 1 \leq D_k \leq N, k = 1, \dots, K \\ & \quad O_k - D_k \leq -2, k = 1, \dots, K \end{aligned} \quad (3.12)$$

3.5 Results

The optimization problem proposed is solved using genetic algorithm (GA). Single objective GA is used when only density estimation accuracy is considered as objective function, and then a multi-objective GA (MOGA) is used to understand the trade-offs between the quality of estimation and operation cost. The MATLAB functions

ga and *gamultiobj* for GA and MOGA, respectively, are used with linear constraints. Settings for both GA and MOGA are summarized in Table 3.2, and the detail of the algorithms can be found in *MATLAB* (2012) and *Deb* (2001) if interested.

Table 3.2: GA and MOGA settings

Parameters	Settings
Chromosome representation	Double vectors
Crossover type	Intermediate
Mutation type	Adaptive Feasible
Crossover rate	0.8
Population size	300
Number of iterations	20

The objective evaluation is focused on the time period between 20 and 90 minute of the overall 3-hour simulated traffic. This optimization time window includes three periods: free flow, increasing traffic, and congestion. Ten probe vehicles are considered in the study ($K=10$), so there are 30 design variables, O_k , D_k , and OT_k , $k = 1, \dots, 10$. Note that even though the optimization focused on time 20-90 minute, vehicles are allowed to be probed any time within the 3-hour traffic. After some preliminary tests on the Newtonian relaxation method using the testing traffic, the parameters of the nudging factor in Equation (3.5) are set as $T_a = 30$ sec, $T_d = 120$ sec, and $X_n = 0.3$ miles.

A baseline scenario is constructed to be compared with optimization results. 10 probe vehicles are evenly distributed in time by starting probing every 7 minutes in the 70-minute optimization time window, and every vehicle is probed for the entire highway stretch. Figure 3.3 shows the trajectories of all the probe vehicles. The evaluated RMSE is 49.68 with the operation cost of \$555 if the operation rate $C=\$1/\text{min}$.

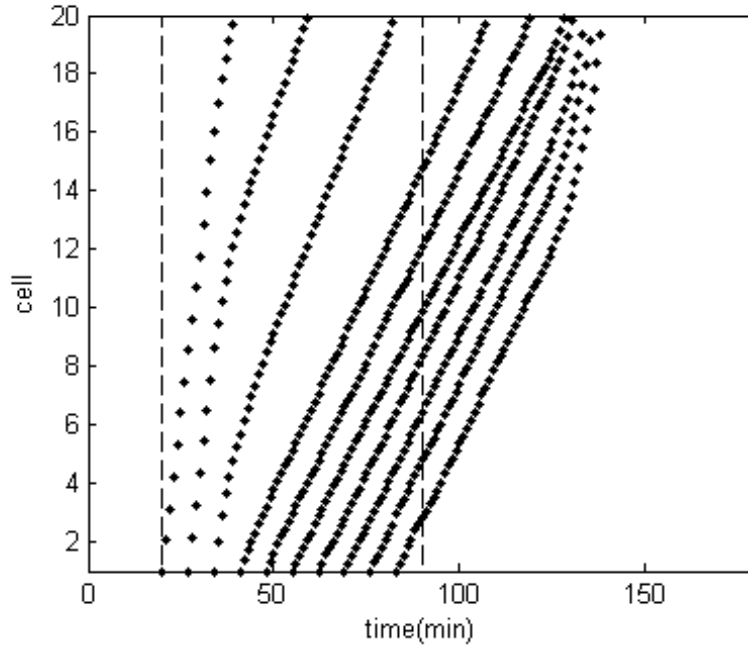


Figure 3.3: Probe vehicle trajectories for baseline scenario

3.5.1 Single Objective: Density Estimation

We first consider only the RMSE as the objective to see what would be the optimal probe vehicle deployment for traffic status estimation regardless of the operation cost. The fitness value converge to 32.9268 after 20 generations as shown in Figure 3.4. Figure 3.5 shows optimal design in the form of probe vehicle trajectories, and the area between the dashed lines indicates the optimization time window where $t = 20-90$. The overall RMSE is 32.93 with operation cost of \$473.46 if the operation rate $C=\$1/\text{min}$. Compared to the baseline scenario, the RMSE has a 34% improvement when the cost is 15 % lower. By comparing the trajectories in Figure 3.3 and 3.5, the optimization allows more even distribution in observation data with shorter trips for some probe vehicles. So both error and cost are improved by the efficient usage of probing data.

The result of density estimation at each loop detector location is shown in Figure 3.6, where the dashed line is the true value measured by the inductive loop detector

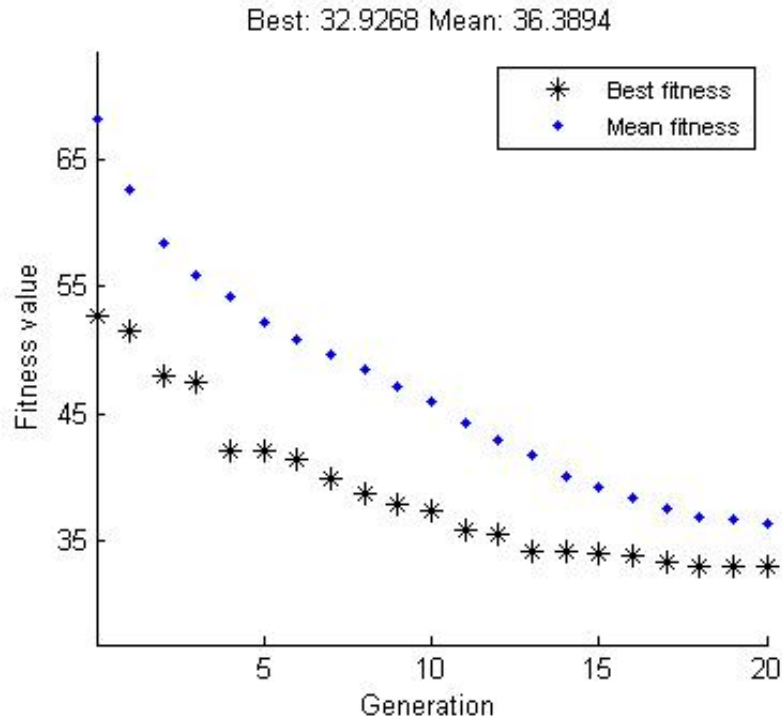


Figure 3.4: Fitness evolution of GA

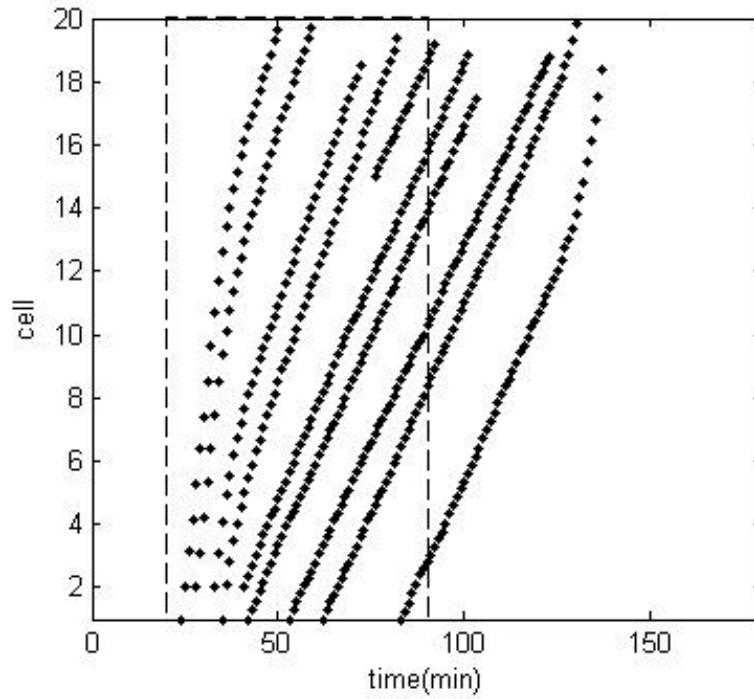


Figure 3.5: Probe vehicle trajectories (GA)

and the solid line is the estimation. The result at loop detector 1 is worse than other stations. The possible reason may be that probing data is sparse at the beginning of the highway section, and the optimum of overall RMSE represents what is good for most of the stations but not all of them. For stations 2 to 6, density is underestimated during the period of increasing traffic. This may indicate that the model have some trouble capture the dramatic traffic increasing during the transition from free flow to congestion. However, the estimation gets better when the traffic reaches the highest congestion level.

3.5.2 Multi-objective: Estimation Error and Operation Cost

Both RMSE and operation cost are considered as objectives, and Figure 3.7 shows the Pareto optimum result from MOGA, where X axis and Y axis represents the fitness value of RMSE and operation cost, respectively. Since better estimation would require more probing data, it is not surprising that the lower cost would harm the accuracy of estimation. However, there are few points distributed almost vertically on the left side of the figure. This suggests that when traffic estimation accuracy is up until a certain level, more probe data collection may only cause higher operation cost but no significant improvement on traffic status estimation.

One point on the Pareto front is chosen to present the results of the design variables and their performance. The RMSE is 34.55, and operation cost is \$283.07 at this chosen optimum. This solution has slightly worse estimation accuracy (5% higher in RMSE) compared to previous optimum from the single-objective GA, but the operation cost has a significant improvement with a 40% decrease. Also, by comparing to the baseline, this chosen optimum has about 30 % improvement in RMSE with only almost half of the probing cost. Probe vehicle trajectories show that many shorter trips are utilized to save operation cost. The density estimation results in Figure 3.9 are similar to Figure 3.6 with only slightly worse performance. When comparing

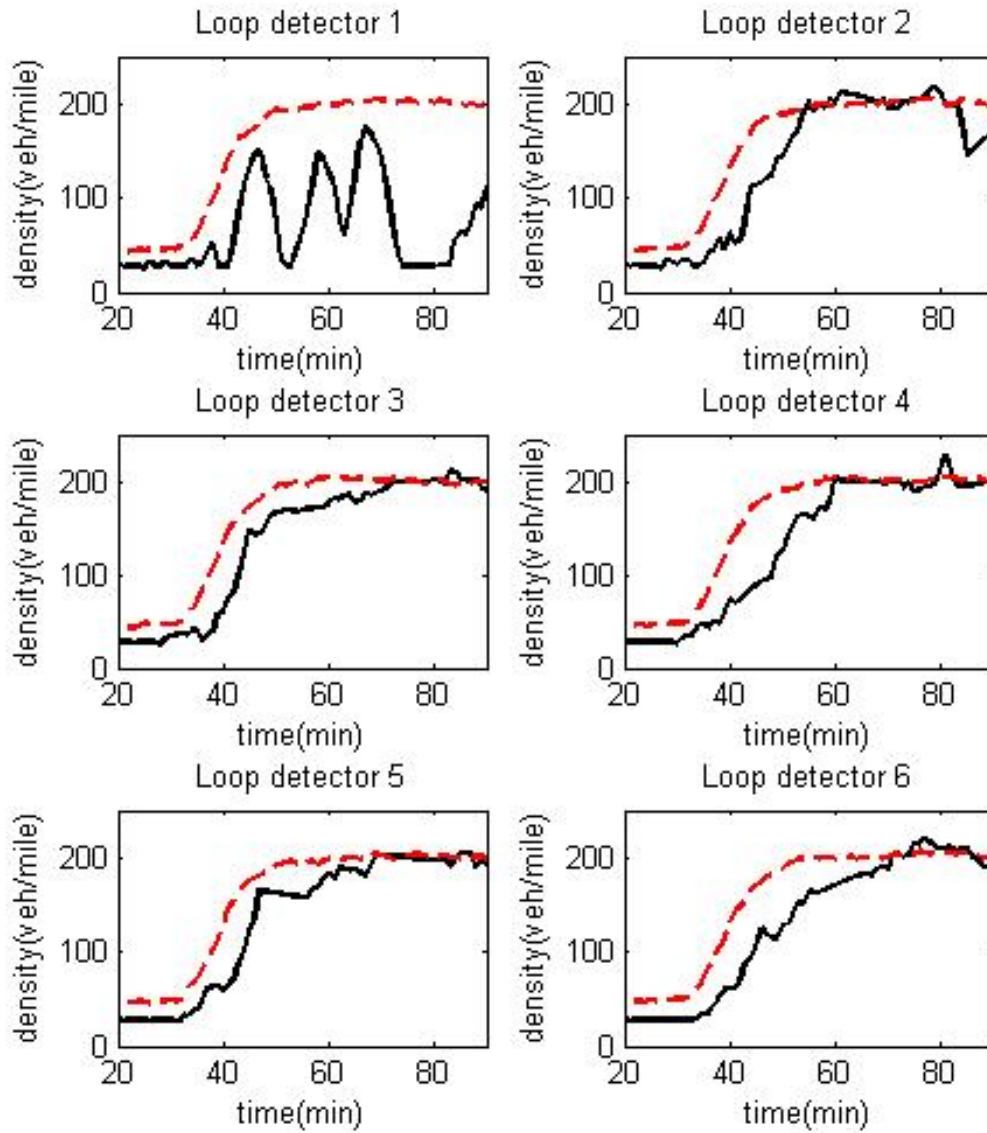


Figure 3.6: Density result from GA

Figure 3.8 to Figure 3.5, probe data is very sparse during congestion period, but the density estimation results are not sacrificed during this period. This can be explained by the nature of the LWR model mentioned in Section 3.2.1 that the model itself is good at modeling congestion condition, so less data is needed to adjust the estimation.

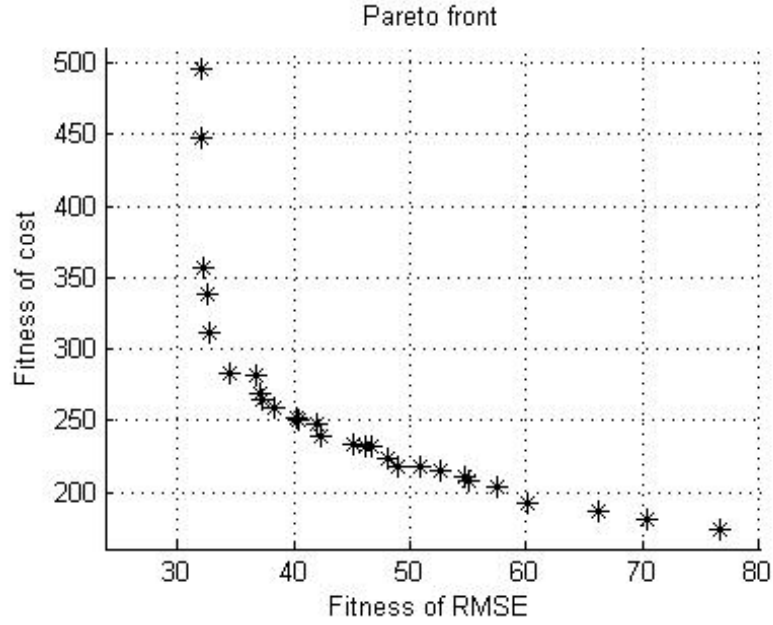


Figure 3.7: Pareto optimum result

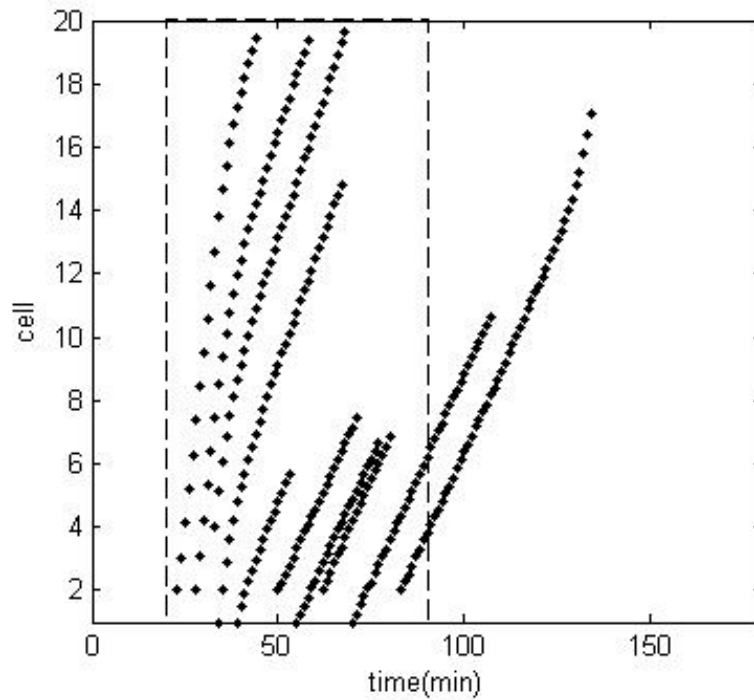


Figure 3.8: Probe vehicle trajectories (MOGA)

3.6 Conclusion

In this section, by incorporating Lagrangian data from probing vehicles using Newtonian relaxation method, an optimization scheme of probe vehicle deployment

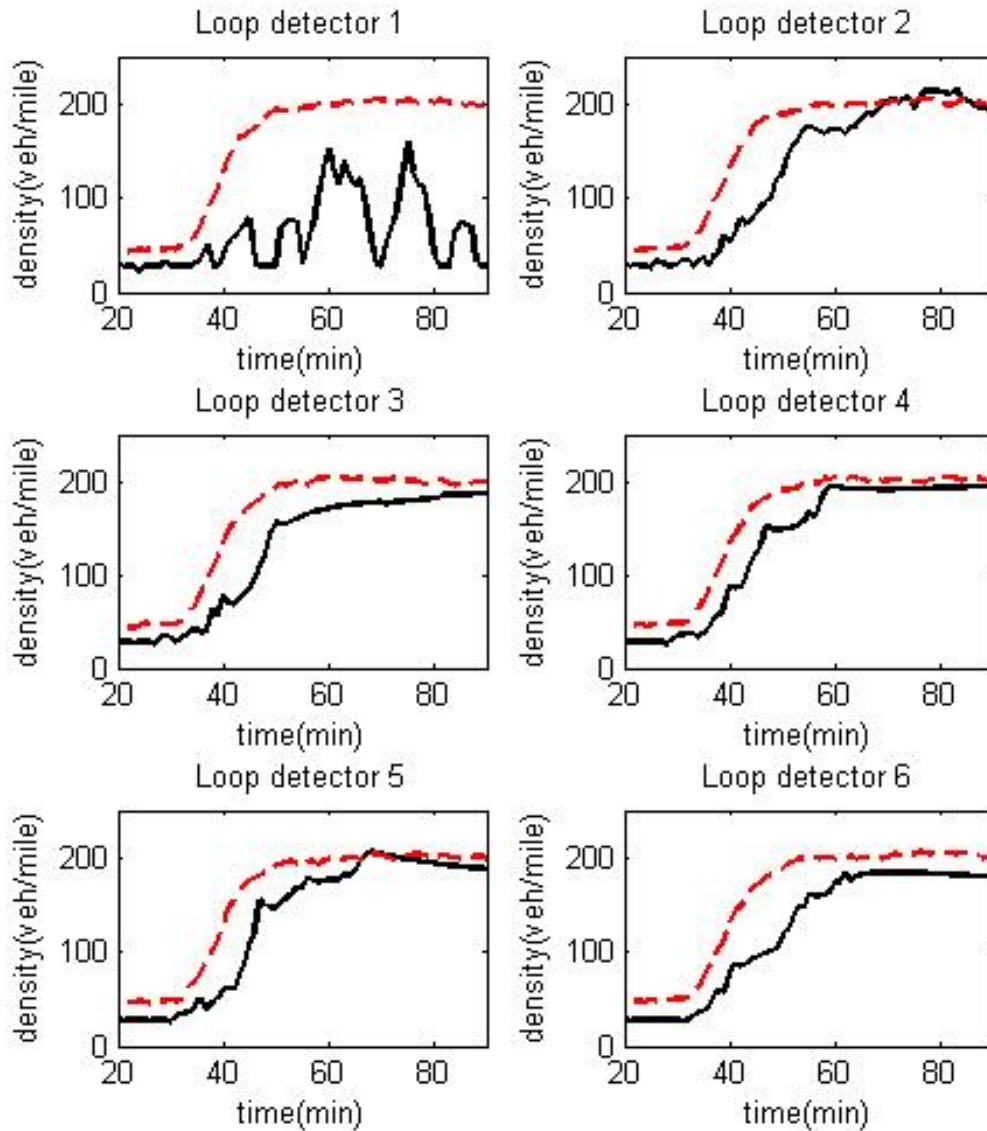


Figure 3.9: Density result from MOGA

was presented by considering the quality of traffic flow estimation and operation cost. This attempt provided insightful information about the trade-off of the information quality and the cost of data. The numerical experiment was done by a simulated traffic based on a stochastic traffic flow model. The result showed that, optimal deployment of probe vehicles can reduce probing cost and estimation error comparing

to the baseline scenario by efficient usage of probe vehicles. By optimizing both probing cost and prediction error, the operation cost could have a 40% decrease with only 5% increase in error comparing to the optimization for prediction error only. So it is possible to decrease probe data for congested traffic with negligible degradation on the quality of traffic status estimation, and the probing strategy should be adaptive with traffic condition. In order to develop a better strategy for the collection and usage of probing data, it is worthwhile to further investigate other data assimilation methods using probing data and a mix of probing and loop detector data. Kalman filter based method may be used for probing data assimilation with real-time application.

CHAPTER IV

Stochastic Lagrangian Traffic Flow Modeling and Real-time Traffic Prediction

4.1 Overview

While Traffic management agency may prefer to use location as the coordinate to know where to implement traffic control strategy to relieve congestion, traffic information follow a platoon of vehicles as in the Lagrangian model is easier to distribute to the drivers inside or near the platoon. The objective of this chapter is to develop a stochastic traffic flow model which 1) uses Lagrangian coordinates to allow utilization of probe vehicle data; 2) can accurately predict traffic status and detect wide moving jam; and 3) update prediction by assimilating data from probe vehicles in real-time. The probing method is to track a pair of vehicles in the traffic, which are identified as the first and last vehicles in a platoon, to collect data of speed and spacing between vehicles. The traffic flow model utilizes unscented Kalman filter (UKF) with dual estimation to update model parameters and estimated current traffic in real-time. The model is validated by empirical highway traffic data from NGSIM project with real-time estimation of current traffic and 3-sec short-term prediction. Another set of traffic data collected by smartphone which has less than 2 % penetration rate with longer time interval is also used to test the scenario with a combination of limited

probing data and loop detector data. Also, a simple adaptive probing scheme is proposed to investigate the benefit of dynamically changing the amount of probing data based on the variance of prediction output from the stochastic model.

4.2 Lagrangian Traffic Flow Model

Like the models shown in Chapter III, most work using the LWR model are formulated in the Eulerian coordinates. Only few efforts focus on the advantages of formulating LWR model in Lagrangian coordinates, such as a theoretical discussion by *Leclercq et al.* (2007) and the work supported by empirical data as in *Yuan et al.* (2012). Instead of the coordinate system (x, t) in space and time, the Lagrangian LWR model use the coordinate system (n, t) , where n is the cumulative count function first proposed by *Newell* (1993). Instead of estimating traffic density, ρ , as used in Chapter III, Lagrangian LWR model uses spacing s to represent traffic state, where $s = 1/\rho$. The LWR model in Lagrangian coordinates can be formulated as in Equation (4.1) with the fundamental diagram in Equation (4.2):

$$\frac{\partial}{\partial t}s(n, t) + \frac{\partial}{\partial n}v(n, t) = 0, \quad (4.1)$$

$$v(n, t) = V^*(s(n, t)). \quad (4.2)$$

The conservation equation in Lagrangian coordinates (4.1) can be explained as the change in average vehicle spacing s in a platoon of vehicles over time t should be the same as the change in speed v over this platoon. The variable n is a number assigned to each vehicle, which decreases in the driving direction. V^* is the fundamental diagram for the relation between vehicle speed and spacing.

Based on the SPDE model with a forcing term on the right-hand-side of the conservation equation as shown in Equation 3.6, a similar stochastic Lagrangian LWR

traffic flow model is proposed in Equation (4.3) with a forcing term as in Equation (4.4):

$$\frac{\partial}{\partial t}s(n, t) + \frac{\partial}{\partial n}v(n, t) = g(n, t), \quad (4.3)$$

$$g(n, t) = \alpha(n, t) + \sigma(n, t) \frac{dW_n(n, t)}{dn \cdot dt}, \quad (4.4)$$

where α and σ are model parameters, and $W(n, t)$ is a Brownian Sheet $W_n(n, t)$ where $E[dW(n, t)] = 0$ and $Var[dW_n(n, t)] = dn \cdot dt$.

4.3 Probing Method and Traffic Data

As mentioned in Section 2.3, fixed-location inductive loop detectors have the disadvantages of high installation cost, difficulty of maintenance and lack of flexibility after installation, and researchers and traffic information providers nowadays are focusing on collecting traffic data from individual vehicles, also known as probing data. Because of the raising interests in probing individual vehicles in the traffic, experiments were conducted to collect vehicle trajectory data for research purpose. The Next Generation Simulation Program (NGSIM) led by Federal Highway Administration (FHWA) provides a real-world dataset with comprehensive traffic data for research, development, and validation of drivers behavior (*US Department of Transportation* (2006)). The data includes trajectories of all the vehicles, vehicle class, speed, lane of traveling, preceding and following vehicles, space and time headways, etc. from multiple highway stretches. Another field experiment called Mobile Century conducted in collaboration by California Center for Innovative Transportation (CCIT), Caltrans, Nokia, and the Department of Civil and Environmental Engineering at University of California, Berkeley utilized GPS-enabled cell phone to collect vehicle trajectory data on the highway (*Herrera et al.* (2010)).

To obtain data from every vehicle in the traffic is very expensive and may not be possible in real life scenario. The data probing should be done in a way which is feasible and convenient for traffic flow model to use. Because of the nature of Lagrangian LWR model, tracking a platoon of vehicles instead of a single vehicle enables the direct calibration of v and s in equation 4.1. We proposed a method to probe a pair of vehicles a reasonable distance apart. By assuming that there are no vehicles entering or leaving this platoon during the period of probing to satisfy the conservation law, the change of distance between the pair reflects the change of average vehicle spacing s in the platoon. Measurements from inductive loop detectors or other fixed-location sensors can be used to provide initial conditions of vehicle counts in the platoon, if the information is not available from probing alone. As illustrate in Figure 4.1, a probing pair, the first and last vehicles in a platoon, is labeled as V_1 and V_2 , the distance between the pair is $x_t^1 - x_t^2$ at time t . Assuming loop detector is available at location x_t^1 , then the number of vehicle in th platoon, Δn , can be measured, and the average spacing at time t can be estimated as in Equation (4.5). After tracking the pair through their trajectory ξ_1 and ξ_2 , the spacing at time $t + \Delta t$ would be as in Equation (4.6).

$$s_t = \frac{x_t^1 - x_t^2}{\Delta n - 1} \quad (4.5)$$

$$s_{t+\Delta t} = \frac{x_{t+\Delta t}^1 - x_{t+\Delta t}^2}{\Delta n - 1} \quad (4.6)$$

4.4 Real-time Traffic

In order to update current traffic state estimation and short-term prediction in real-time by newly collected traffic data, a recursive data assimilation method is required for this update. In this section, we explain the basic idea of Kalman filter

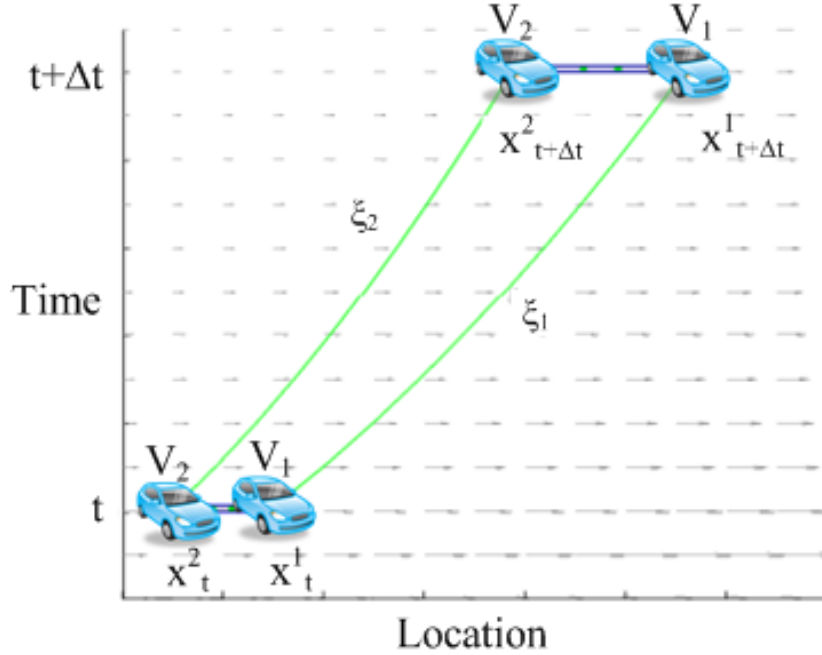


Figure 4.1: Probing vehicles in pair

method and the nonlinear Kalman filter, UKF, which is used to update the model parameters and the traffic status estimation with the proposed Lagrangian traffic flow model.

4.4.1 Kalman Filter Method

Kalman filtering (*Kalman et al.* (1960)) is a recursive method which uses a series of noisy measurements observed over time to produce a statistically optimal estimation of the underlying system state. The algorithm works in a two-step process. Consider the system has state variable x_t at time t , and the state space model can be written as:

$$x_t = F_t x_{t-1} + w_t \quad (4.7)$$

$$y_t = H_t x_t + \epsilon_t \quad (4.8)$$

where y_t is the observation variable with measurement noise $\epsilon_t \sim N(0, Q_t)$. $w_t \sim N(0, R_t)$ is the process noise, and F_t and H_t are state transition model and observation model, respectively.

The Kalman filter first produces estimates of the current state variables, the priori estimation of the state $x_{t|t}$ and priori error covariance matrix $P_{t|t-1}$. Once the outcome of the next measurement is observed, these estimates are updated to obtain the posteriori distribution of the state, $x_{t|t}$ and $P_{t|t}$. The process is formulated as below:

Prediction:

$$\begin{aligned} x_{t|t-1} &= F_t x_{t-1|t-1} \\ P_{t|t-1} &= F_t P_{t-1|t-1} F_t^T + R_t \end{aligned} \tag{4.9}$$

Update:

$$\begin{aligned} z_t &= y_t - H_t x_{t|t-1} \\ S_t &= H_t P_{t|t-1} H_t^T + R_t \\ K_t &= P_{t|t-1} H_t^T S_t^{-1} \\ x_{t|t} &= x_{t|t-1} + K_t z_t \\ P_{t|t} &= (I - K_t H_t) P_{t|t-1} \end{aligned} \tag{4.10}$$

where K_t is the optimal Kalman gain, z_t is the measurement residual with covariance S_t .

Kalman filter gives the optimal estimation for linear space model, but the stochastic traffic flow model such as the proposed stochastic traffic flow model has F_t nonlinear. Therefore, nonlinear Kalman filter has to be used. Previous work mentioned in Section 2.4 have used various nonlinear filtering algorithm for real-time application, and here the Unscented Kalman filter (UKF) will be discussed next.

4.4.2 Unscented Kalman Filter

Unscented Kalman filter (UKF) proposed by *Julier and Uhlmann* (2004) uses a mathematical sampling technique called unscented transform to estimate the mean

and covariance of the output variable from a nonlinear transformation of the input variable. UKF first generate a set of weighted sample points, also called sigma points, from mean μ and covariance matrix P of the input random variable by using unscented transform. Each sigma point is considered as a realized input of the nonlinear function. And then the mean and covariance of the output variable can be estimated by the sample output obtained from those sigma points. The i th sigma point χ^i produced by unscented transformation is shown in Equation (4.11):

$$\begin{aligned}\chi^0 &= \mu \\ \chi^i &= \mu - (\sqrt{(L + \lambda)P})_i, i = 1, 2, \dots, L \\ \chi^{L+i} &= \mu - (\sqrt{(L + \lambda)P})_{i-L}, i = 1, 2, \dots, L\end{aligned}\tag{4.11}$$

where L is the dimension of state variable, and λ is determined by Equation (4.12) with parameters α and κ to control the spread of sigma points.

$$\lambda = \alpha^2(L + \kappa) - L\tag{4.12}$$

The mean and covariance for output variable are approximated using a weighted sample mean and covariance of the sigma points, with the corresponding weight for mean W_m^i , and the weight for covariance W_c^i of each sigma point χ^i are:

$$\begin{aligned}W_m^0 &= \frac{\lambda}{\lambda + L} \\ W_c^0 &= \frac{1}{2(\lambda + L)} + (1 - \alpha^2 + \beta), i = 1, 2, \dots, L \\ W_m^i &= W_c^i = \frac{1}{2(\lambda + L)}, i = 1, 2, \dots, L\end{aligned}\tag{4.13}$$

where β is another parameter to incorporate prior knowledge of the distribution of the input variable.

In order to independently estimate model parameters and traffic state in terms of vehicle spacing, dual UKF estimation is used in the real-time traffic model. Model

parameters are estimated first by using previous estimation of traffic status as a constant. After performing UKF to estimate parameters, the traffic status can be estimated by using the updated estimation of model parameters with UKF. The complete state space model is explained next, followed by a detailed explanation of a dual UKF iteration.

4.4.3 State Space Models

The model has two sets of state variable: parameters in the traffic flow model and the traffic status in every probed cell (platoon of vehicles) at each time step. Model parameters α and σ in all the cells on the highway stretch at time t can be represented in a vector form as in Equation (4.14):

$$\mathbf{p}_t = [\alpha_t^1, \sigma_t^1, \dots, \alpha_t^i, \sigma_t^i, \dots, \alpha_t^N, \sigma_t^N]^T. \quad (4.14)$$

By assuming that the state transition of model parameters follows a random walk with a normal distributed ϕ_t , the state transition equation for \mathbf{p}_t can be written as in Equation (4.15)

$$\mathbf{p}_t = \mathbf{p}_{t-1} + \phi_t. \quad (4.15)$$

And the state variable for traffic status is a vector of the spacing in all the cells on the highway stretch as in Equation (4.16):

$$\mathbf{s}_t = [s_t^1, \dots, s_t^i, \dots, s_t^N]^T. \quad (4.16)$$

The state transition for \mathbf{s}_t follows the Lagrangian LWR model, which can be represented as in Equation (4.17)

$$\mathbf{s}_t = f(\mathbf{s}_{t-1}, \mathbf{p}_t, \boldsymbol{\omega}_t), \quad (4.17)$$

where $\boldsymbol{\omega}_t$ is an independent zero-mean Gaussian noise.

For the observation equation, the vehicle spacing can be directly observed, so the observation equation is simply

$$\mathbf{y}_t = h(\mathbf{s}_t, \boldsymbol{\epsilon}_t) = \mathbf{s}_t + \boldsymbol{\epsilon}_t, \quad (4.18)$$

where \mathbf{y}_t is the vector of observed vehicle spacing of all the cells at time t , and $\boldsymbol{\epsilon}_t$ is an independent zero-mean Gaussian noise.

4.4.4 Estimation of Current Traffic State and Traffic Prediction

The iteration of using dual UKF to estimate current traffic status and predict future traffic is presented as the following:

1. Initialization – Initialize posteriori estimation of state $\hat{\mathbf{s}}_0$, $\hat{\mathbf{p}}_0$ and error covariance matrix \mathbf{Q}_0^s and \mathbf{Q}_0^p with Equation (4.19). And then set $t = 1$.

$$\begin{aligned} \hat{\mathbf{s}}_0 &= E[\mathbf{s}_0] \\ \hat{\mathbf{p}}_0 &= E[\mathbf{p}_0] \\ \mathbf{Q}_0^s &= E[(\mathbf{s}_0 - \hat{\mathbf{s}}_0)(\mathbf{s}_0 - \hat{\mathbf{s}}_0^T)] \\ \mathbf{Q}_0^p &= E[(\mathbf{p}_0 - \hat{\mathbf{p}}_0)(\mathbf{p}_0 - \hat{\mathbf{p}}_0^T)] \end{aligned} \quad (4.19)$$

2. Update model parameters – Use $\hat{\mathbf{s}}_{t-1}$ as a constant and plug into state transition Equation (4.15) and the observation equation (4.20) below, and use UKF to update $\hat{\mathbf{p}}_t$, \mathbf{Q}_t^p by considering only \mathbf{p}_t as the state variable.

$$\mathbf{y}_t = h(f(\hat{\mathbf{s}}_{t-1}, \mathbf{p}_t, \boldsymbol{\omega}_t), \boldsymbol{\epsilon}_t), \quad (4.20)$$

3. Update traffic status – Use $\hat{\mathbf{p}}_t$ as a constant and plug into state transition equation (4.17) and the observation equation (4.18), and use UKF to update $\hat{\mathbf{s}}_t$, \mathbf{Q}_t^s by considering only \mathbf{s}_t as the state variable.
4. Prediction (skip when estimating current traffic state only) – Repeat Step 2 to predict model parameters, and then predict traffic state with Equation (4.15) until prediction time without observation.
5. Set $t = t + 1$, go to Step 2.

4.5 Result from NGSIM Data

In this section we first present the observation from NGSIM data on US-101 Southbound regarding traffic phases. Then, we use the result of real-time estimation and prediction to show the capability of the stochastic Lagrangian LWR model. We also discuss how the parameter α can be used to detect the phase change of wide moving jam.

4.5.1 Traffic data and Traffic Phases on US-101

The Next Generation SIMulation (NGSIM) program using cameras to record traffic on a segment of US-101 (Hollywood Freeway) in Los Angeles, California on June 15, 2005. Software is used to detect and track vehicles in a 2100-ft long study area. Data is processed and becomes available in three 15-minute segments between 7:50

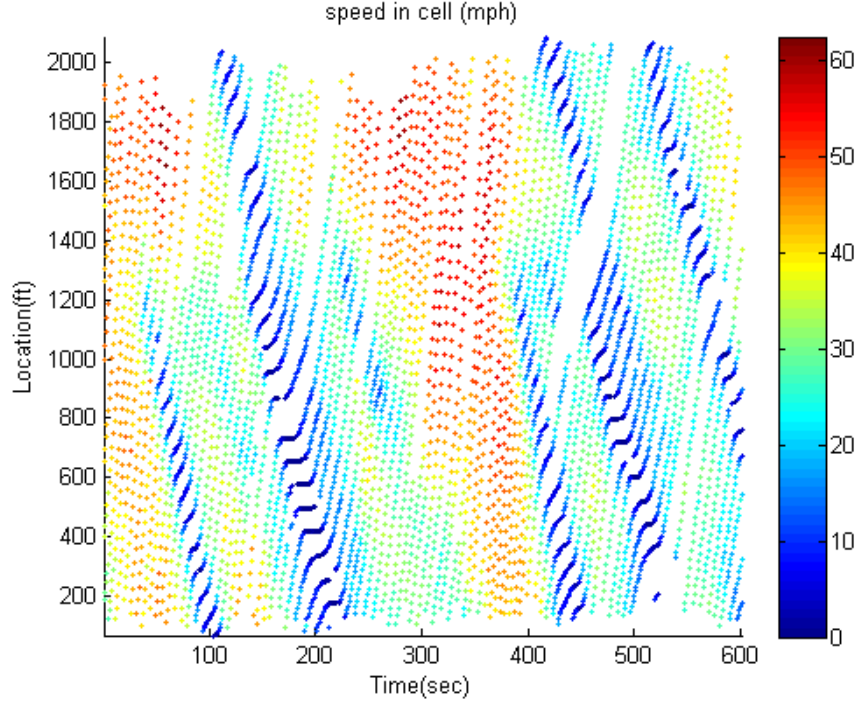


Figure 4.2: Average speed in each cell on US-101

am and 8:35 am, with a time interval of 0.1 sec. The highway stretch has a speed limit of 55 mph, with 5 lanes and an auxiliary lane, and only data from the inner most lane is used for this study.

While NGSIM data collects trajectory of every vehicles with time interval of 0.1 sec, the probing is done by tracking the first and last vehicle from a cell of 3 vehicles with the sample time of 1 sec. 10 minutes of data is used as the training set to find the fundamental diagram V^* in Equation (4.2) for the traffic, and then another 10 minutes of the data is used to evaluate the performance of the model. Because of the stochasticity observed in the training set, a power function with a Gaussian noise, θ is used as the fundamental diagram, which is shown in Equation (4.21) below:

$$v = V^*(s) = a \cdot s^b + c + \theta, \quad (4.21)$$

where parameters $a = -296.55$, $b = -0.45$, and $c = 74.80$.

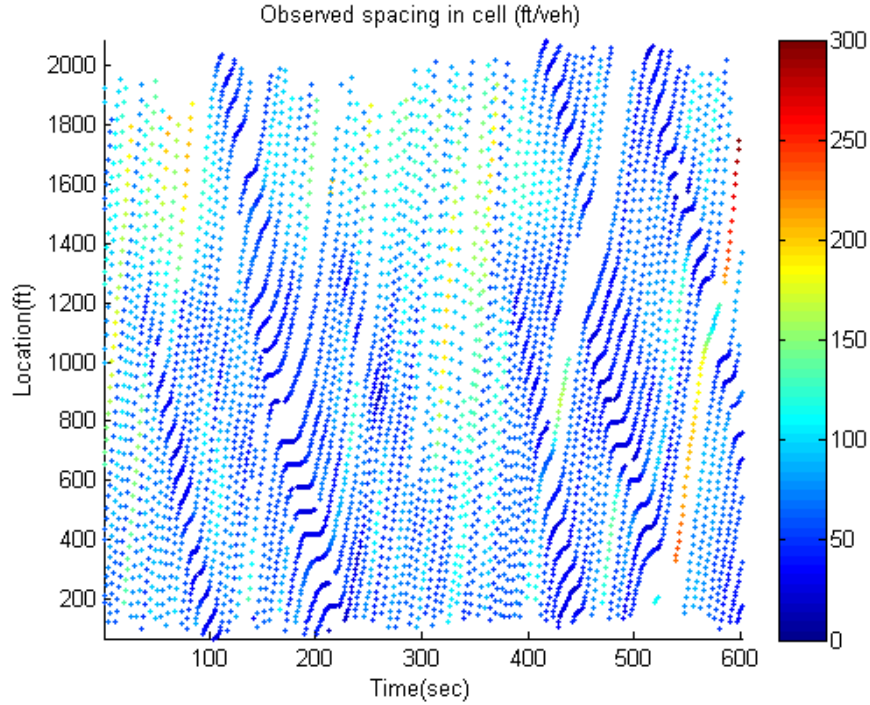


Figure 4.3: Observation of traffic state in each cell on US-101

We first exam the traffic phases in the testing set, and the average speed of each cell can be found in Figure 4.2. Multiple incidents of wide moving jam can be clearly observed in the figure with the low speed region (dark blue, approximated below 6 mph) traveling backwards in space with time.

4.5.2 Real-Time Estimation of Current Traffic State

The average spacing between vehicles in each cell can be found by knowing the distance between the first and the last vehicles and the vehicle count of each cell. The observed spacing is presented in Figure 4.3. By using the model in Equation (4.3) and (4.4) and UKF explained in Section 4.4 for updating the model parameters and spacing in real-time, the result of estimated spacing of current traffic (average of 10 runs) is shown in Figure 4.4. By visually comparing both figures, the estimation of traffic state follows the observed traffic pattern very well. Estimation error calculated by RMSE (root mean square error) and MAPE (mean absolute percentage

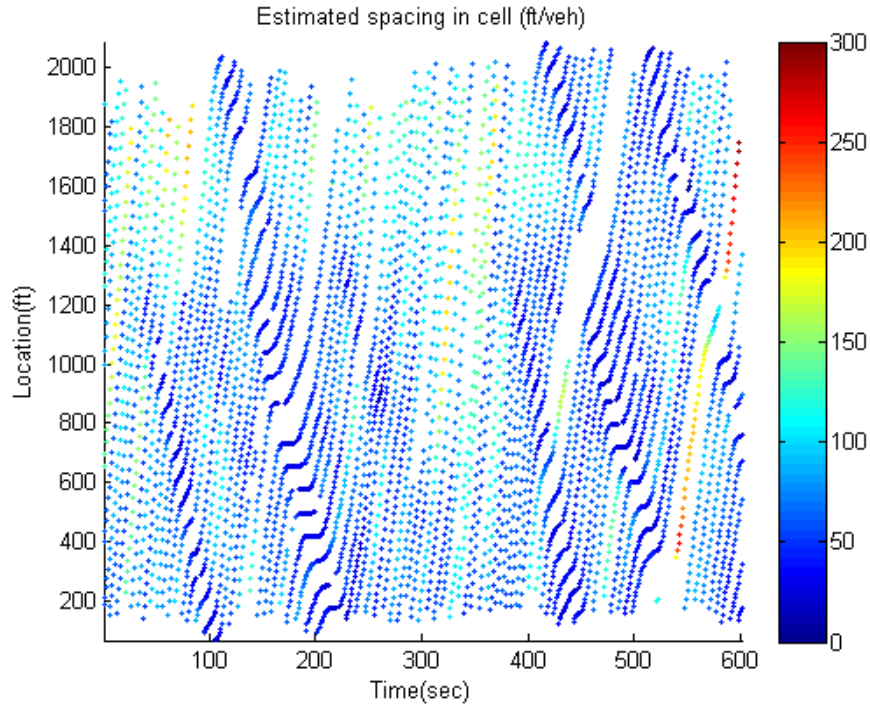


Figure 4.4: Estimation of current traffic state in each cell on US-101

error) are summarized in Table 4.1 with overall and a separation of wide moving jam and non-jam traffic. Because the spacing during jam phase is much smaller than non-jam, RMSE during jam can be lower due to the scale of spacing, and MAPE may provide a more reasonable comparison between jam and non-jam traffic. By comparing the stochastic Lagrangian LWR model with the deterministic Lagrangian LWR model, both models perform better in estimating non-jam traffic than jam. The result shows that using a stochastic model with real-time updating can have an overall 20% improvement comparing to the estimation from deterministic model, and the improvement is even higher for jam traffic (about 27%).

4.5.3 Prediction of Traffic State

Future traffic prediction is also performed to predict traffic state 3-sec ahead. While the observation data updates the model parameters and estimation of current spacing, the traffic flow model predict the model parameters and future traffic status

Table 4.1: Error of average spacing estimation of current traffic state on US-101

Deterministic Lagrangian LWR			
	Overall	Non-jam	Jam
RMSE(ft)	6.13	6.28	4.47
MAPE(%)	7.9	7.6	10.9
Stochastic Lagrangian model			
	Overall	Non-jam	Jam
RMSE(ft)	5.06	5.20	3.32
MAPE(%)	6.3	6.1	8.0

Table 4.2: Error of 3-sec prediction of spacing on US-101

Deterministic Lagrangian LWR			
	Overall	Non-jam	Jam
RMSE(ft)	17.85	18.10	15.30
MAPE(%)	23.2	22.0	35.3
Stochastic Lagrangian model			
	Overall	Non-jam	Jam
RMSE(ft)	12.26	12.49	9.77
MAPE(%)	15.4	14.6	22.9

in the next 3 second. As expected, the prediction error is higher than the estimation of current traffic state when comparing Table 4.2 to Table 4.1. The stochastic model has significantly better prediction, which is about 35% lower in MAPE than the deterministic model. By examining the absolute percentage error of the prediction from stochastic model along the trajectory of each cell in Figure 4.5, it shows that most of the higher error occur when the traffic is at the transition to wide moving jam. This result shows that the stochastic model can provide short-term prediction to foresee the traffic pattern in general, but it may be difficult to precisely predict the timing of phase transition if only relying on the traffic state variable (spacing).

4.5.4 Wide Moving Jam Detection

In order to explore other ways to detect traffic phase changes, Figure 4.6 shows the right-hand-side of Equation (4.1) from the observation data. It shows that RHS

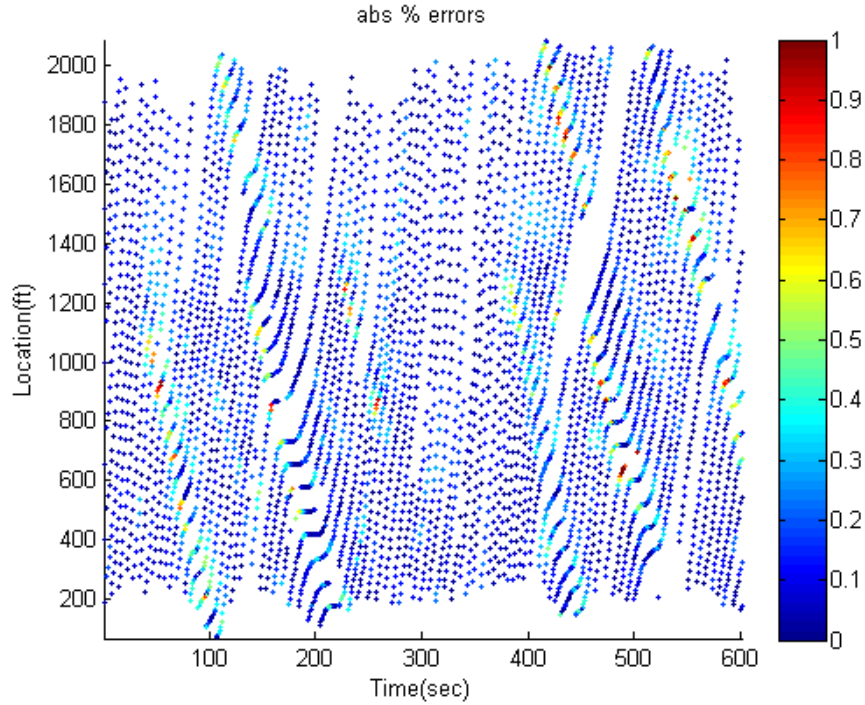


Figure 4.5: Absolute percentage error of 3-sec prediction in spacing on US-101

continuously decreases when a cell is approaching jam traffic, and RHS reaches minimum value right before entering a jam. RHS dramatically increase to around zero during the jam, and then jump to a larger positive value when the cell leaves the jam region. Therefore, the estimation of model parameter α in the forcing function of Equation (4.4) could be used as an indicator of the potential phase change to wide moving jam.

Figure 4.7 is the result of estimated α of current traffic state, which shows similar pattern as RHS in Figure 4.6. In the case of using -10 ft/veh/sec as the threshold value for α , it can predict wide moving jam with an average lead time of 6.76 sec (approximately 250 ft from the jam when speed is at 25 mph). 75% of the chance that when the estimated α reaches -10 or lower, the cell will reach a jam in 1-25 sec, and 63% of the wide moving jam identified in Figure 4.2 can be detected by α before the jam occurs. Therefore, the estimated α can be used solely or combining with short-term prediction of traffic state to detect wide moving jam in advance.

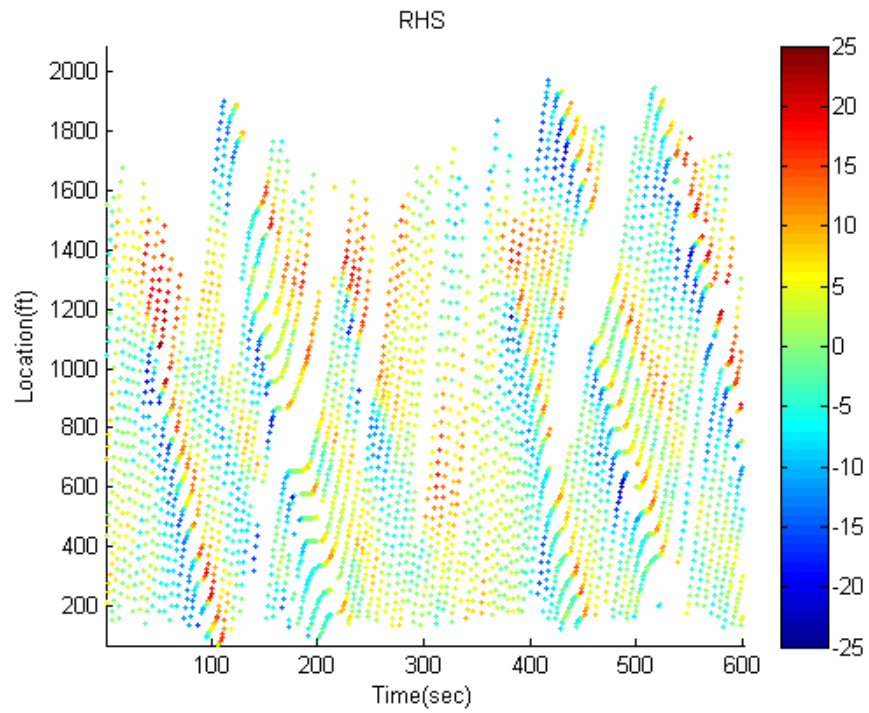


Figure 4.6: Observed right-hand-side of Lagrangian LWR model (ft/veh/sec)

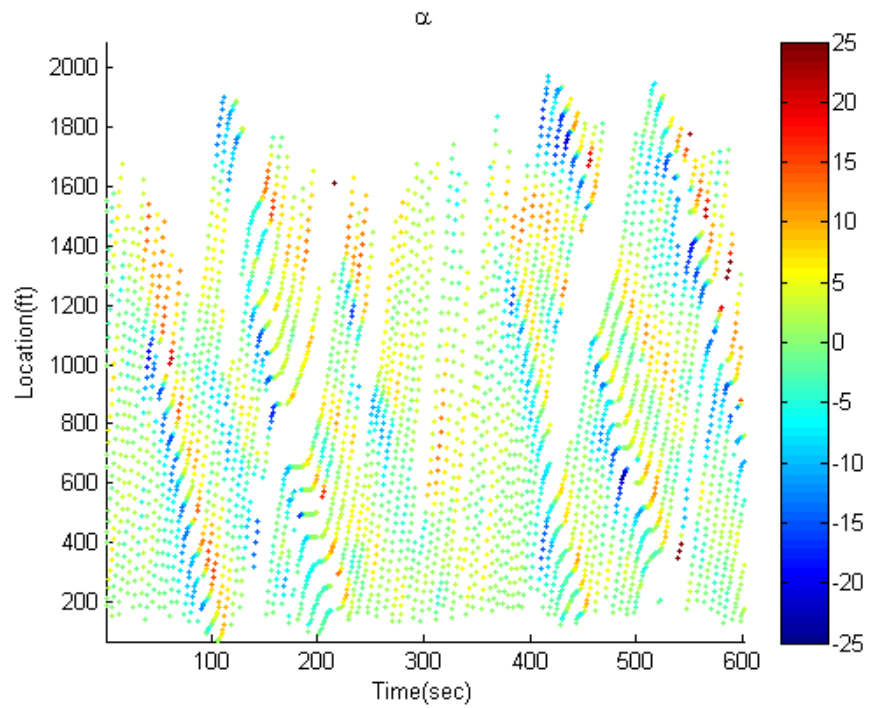


Figure 4.7: Estimated α of current traffic state (ft/veh/sec)

4.6 Result from Mobile Century Data

The NGSIM data used in the previous section has complete information with high resolution, which allows the probing to be evenly distributed in the traffic. However, in reality, such a comprehensive data may not be available. Also, the length of NGSIM data was limited by a short time period and a half-mile highway stretch. In this section, the scenario where probing pairs are scarce and the vehicle counts in each cell are varied will be examined with data collected by Mobile Century Experiment, which contains a longer highway stretch with hours of data.

4.6.1 Traffic data and Traffic Phases on I-880

The Mobile Century Experiment is a filed experiment conducted on February 8th, 2008 by University of California, Berkeley and other collaborators. 100 probe vehicles equipped with GPS-enabled Nokia N95 smart phones were driving repeatedly in loops of 6-10 miles on freeway I-880 near Union City in the San Francisco Bay Area, California. About 2200 trips were generated between 9:30am and 6:30pm. Geo-position of each vehicle is collected by the phone every 3 sec, and flow rate and occupancy data from each lane are collected by about 17 loop detectors every 30 sec.

Northbound data from 2:30 pm to 5:30 pm are used in this study with about 6 miles of traffic. Trips are probed in pairs only when spacing is between 20 and 1000 ft. Because the number of vehicle between each probing pair is unknown, loop detector data is used to estimate the cell size of each probing pair (cell). Timestamps are recorded when two probing vehicles passing the same loop detector, and the flow rate recorded between the two timestamps is aggregated and averaged across all the lanes to obtain the estimated cell size of the probing pair. And then, the average spacing between two vehicles in the cell can be calculated.

The traffic phases can first be observed by examining the average speed of each cell as shown in Figure 4.8. A bottleneck at postmile 24.5 causes the synchronized flow

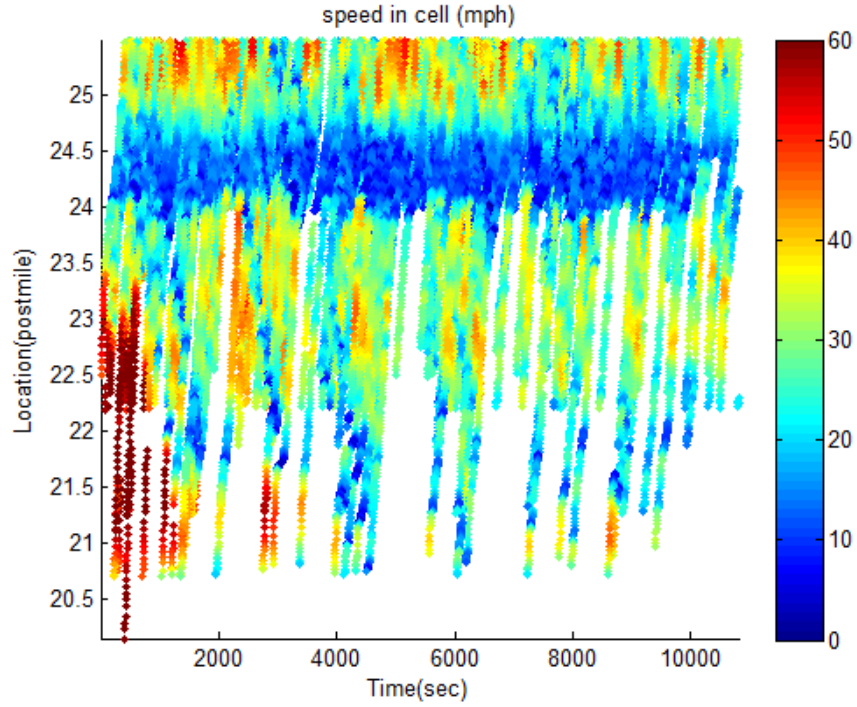


Figure 4.8: Average speed in each cell on I-880

between postmile 24 and 24.5. Multiple incidents of slowing down can be observed in the figure which travel backwards in time and space, within and outside of the synchronized flow region, so they satisfy the characteristics of wide moving jam.

Table 4.3: Error of average spacing estimation of current traffic state on I-880

Deterministic Lagrangian model			
	Overall	Non-jam	Jam
RMSE(ft)	58.42	60.24	36.11
MAPE(%)	27.9	27.1	35.7
Stochastic Lagrangian LWR			
	Overall	Non-jam	Jam
RMSE(ft)	48.98	50.66	27.74
MAPE(%)	19.3	19.4	17.9

4.6.2 Estimation and Prediction of Traffic State with Scarce Probing Data

Estimation error calculated by RMSE and MAPE are summarized in Table 4.3 with overall and a separation of wide moving jam and non-jam traffic. Compare to the result in Table 4.1, the information accuracy suffered when the amount of probing data decreased. While data used in Section 4.5 has 1-sec time interval and evenly distributed probing vehicles with about 65 % penetration rate, Mobile Century data has larger time step (3 sec), a much lower penetration rate (no more than 2%), with the uncertainty in the estimation of cell size using loop detector data. The stochastic model maintains around 19 % in MAPE overall, which is about 30 % improvement from the deterministic model.

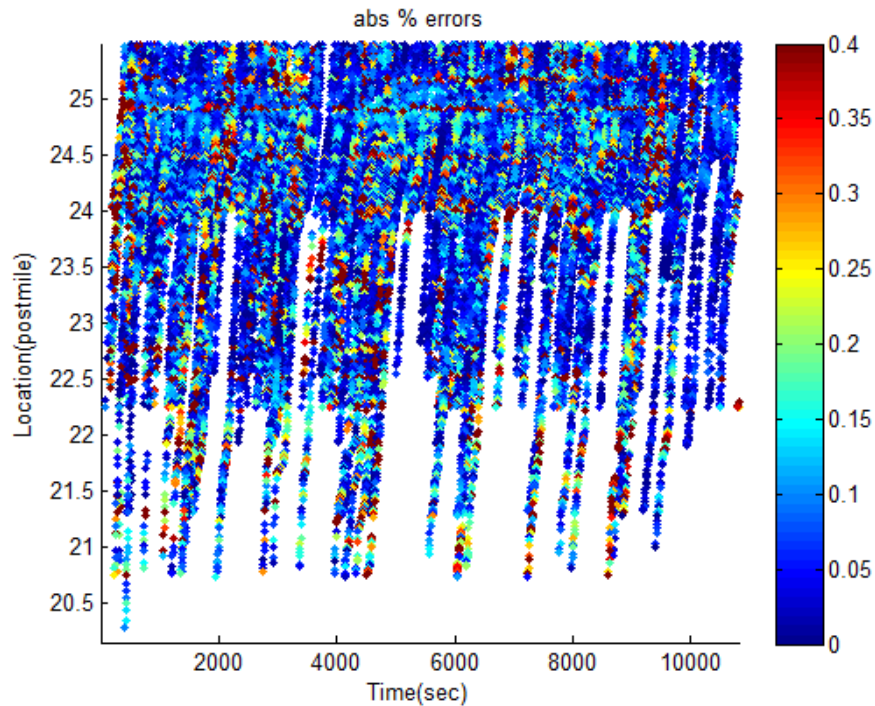


Figure 4.9: Estimation error in each cell on I-880

The absolute percentage error in time and space domain in Figure 4.9 does not seem to be related to traffic state. However, some of the high error points seem to

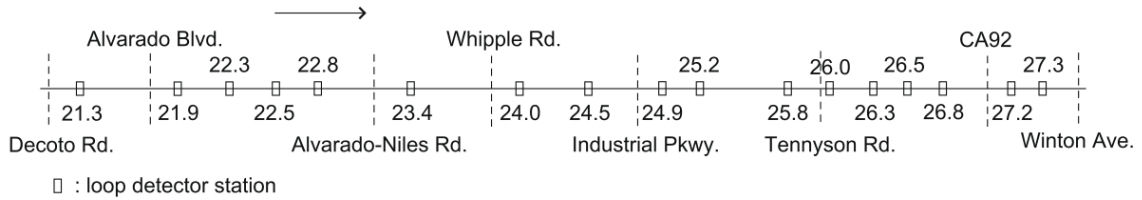


Figure 4.10: Loop detector location on I-880 (*Herrera et al. (2010)*)

line up at loop detector locations as marked in Figure 4.10, such as milepost 24.5 and milepost 24.9. Since loop detector data is only used to estimate cell size, we then look into the estimated cell size in Figure 4.11. While the cell size is in a range approximately 2 to 75, extremely small cell size may suggest that the two probing vehicles are not in the same lane, and extremely large cell size means the two vehicles are too far away from each other. Also, some dramatic changes in cell size can be observed when the estimation gets updated by data from the next loop detector. This suggests that the error in cell size estimation could have a significant impact on the accuracy of the traffic status estimation. Also, because GPS information does not reveal in which lane the vehicle is traveling on a 4-lane highway, the tracking pair may be traveling in different lanes with slightly different congestion level. Therefore, if more information can be obtained from the data to allow the probing process to select pairs that travel on the same lane with a reasonable spacing, the cell size may be better estimated to allow better prediction of the traffic.

Future traffic prediction is also performed to predict traffic state 9 sec (3 time steps) ahead, and the result is reported in Table 4.2. Prediction results in poor accuracy when data is scarce and limited, but stochastic model is still, in general, improving the prediction error by about 28 % comparing to the deterministic model.

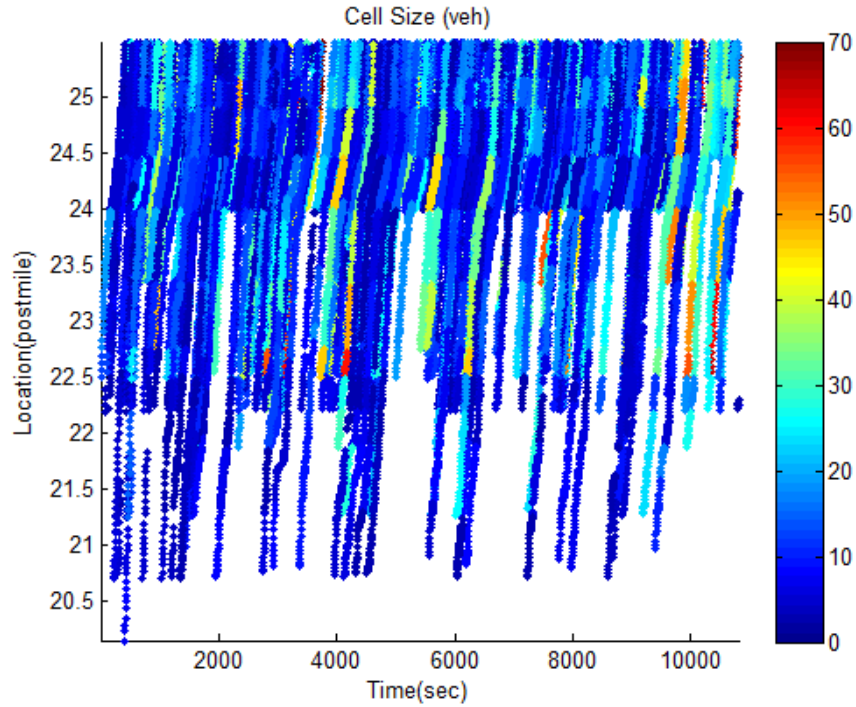


Figure 4.11: Estimated cell size in each cell on I-880

4.6.3 Wide Moving Jam Detection with Scarce Data

The same method of using the estimated α value to detect wide moving jam is also attempted with Mobile Century data. By using -5 ft/veh/sec as the threshold value for α , it can predict wide moving jam with an average lead time of 14 sec (approximately 410 ft from the jam when speed is at 20 mph). However, only 25% of the chance that when the estimated α reaches -5 or lower, the cell will reach a jam. And 50% of the wide moving jam identified in the traffic can be detected by α before the jam occurs. When the data is limited and the estimation accuracy is low, α could change irregularly in some cells, which cause many false alerts in this case.

4.7 Adaptive Probing

While the variance from multiple simulation runs of the stochastic traffic flow model can be considered as the reliability of the mean value of the predicted result,

Table 4.4: Error of 9-sec prediction of spacing on I-880

Deterministic Lagrangian LWR			
	Overall	Non-jam	Jam
RMSE(ft)	111.28	115.06	63.58
MAPE(%)	63.2	62.7	68.4
Stochastic Lagrangian model			
	Overall	Non-jam	Jam
RMSE(ft)	88.93	91.57	57.10
MAPE(%)	45.5	45.5	46.3

it is possible to adaptively adjust probing strategy based on the variance to improve the quality of traffic prediction. A simple way to do adaptive probing is to change the number of probing samples from the traffic, which can be represented by the number of vehicle in a cell. When the predicted traffic status indicates high variation from the stochastic model, the cell size can be smaller to collect more probing data from the same highway stretch.

The flow chart in Figure 4.12 is used to describe the proposed adaptive probing scheme. The default probing setting is tracking the first and last vehicles of a cell of 6 vehicles. When the standard deviation from random seeded simulation runs exceed a threshold value σ_{limit} , or when tracking in a cell of 6 is infeasible at some point, the model then request for additional data to allow a cell of 3 vehicles. For the case that both cell of 3 and cell of 6 are providing prediction result, the model would choose the prediction with lower standard deviation to allow the information with better confidence.

The same data set in Section 4.6.1 is used to perform the testing with standard deviation from 30 runs with 3-sec prediction. The volume of data is calculated by the total number of tracked data entries. The performance is evaluated by MAPE for the entire traffic. MAPE is calculated by assuming all the vehicles in the same cell share the same predicted spacing, and the predicted spacing is compared with observed space headway of each vehicles in the cell. Figure 4.13 and Figure 4.14 are

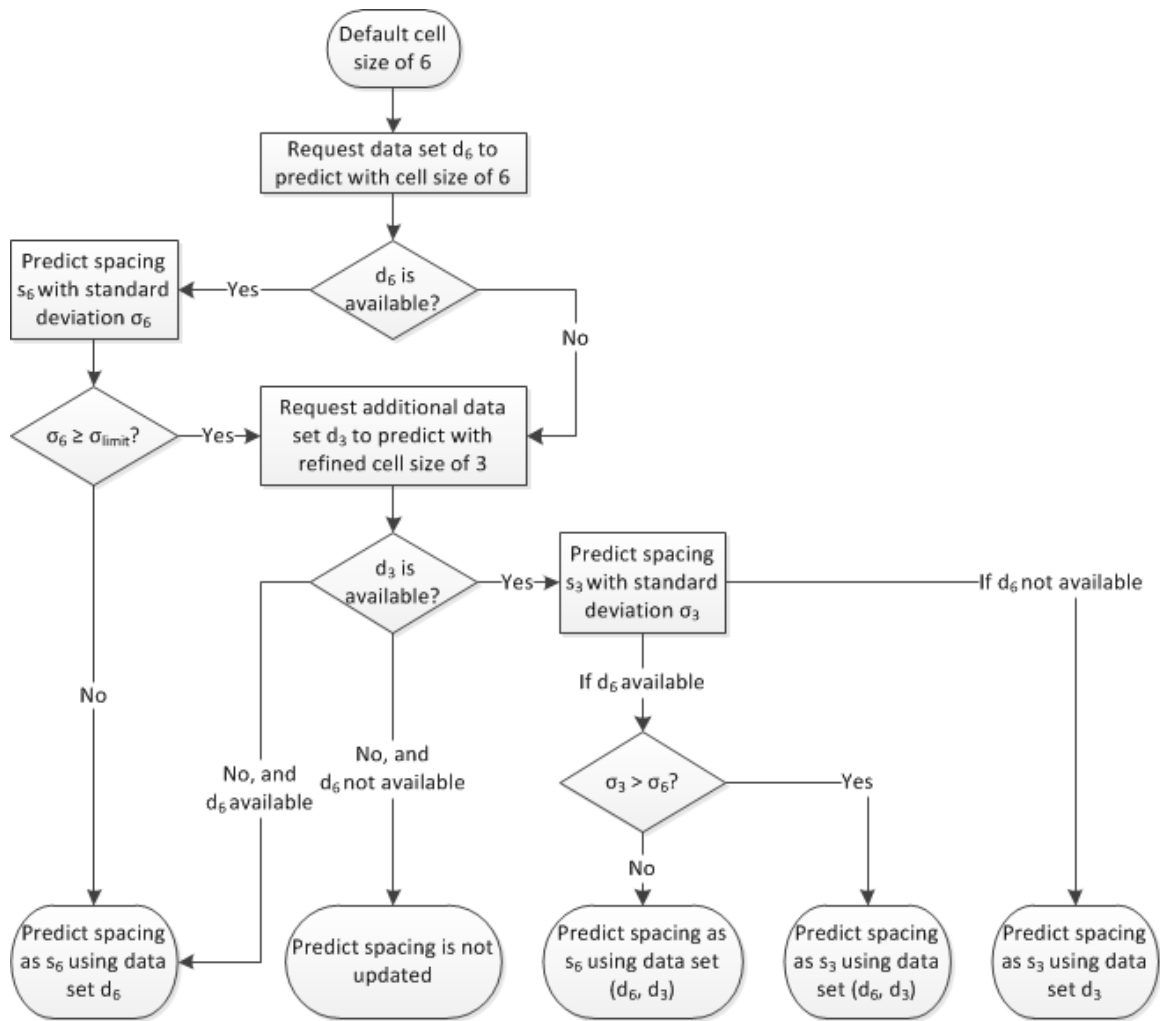


Figure 4.12: Flow chart for adaptive probing

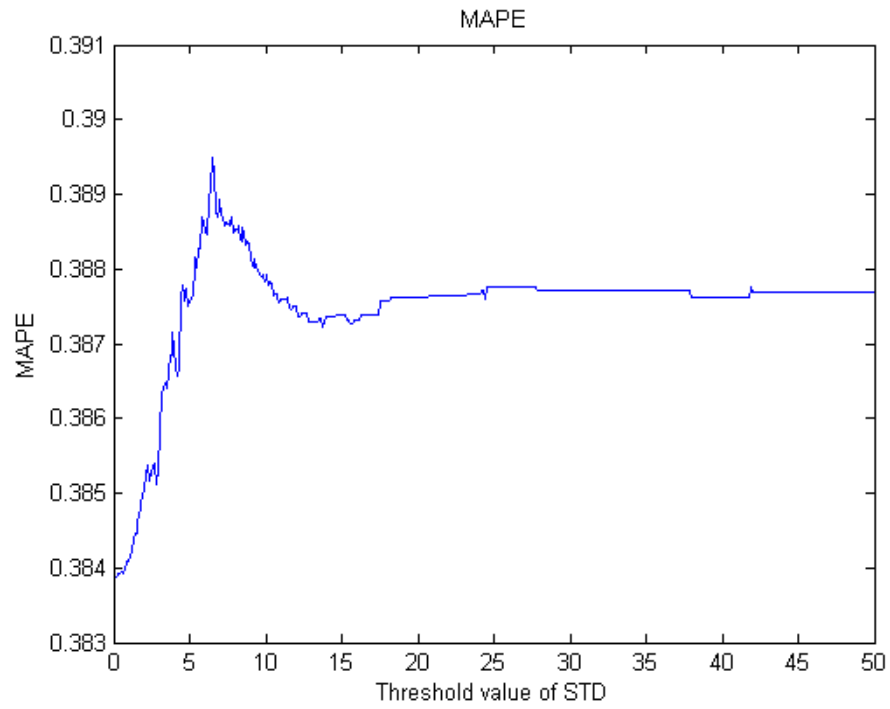


Figure 4.13: Mean absolute percentage error of adaptive probing

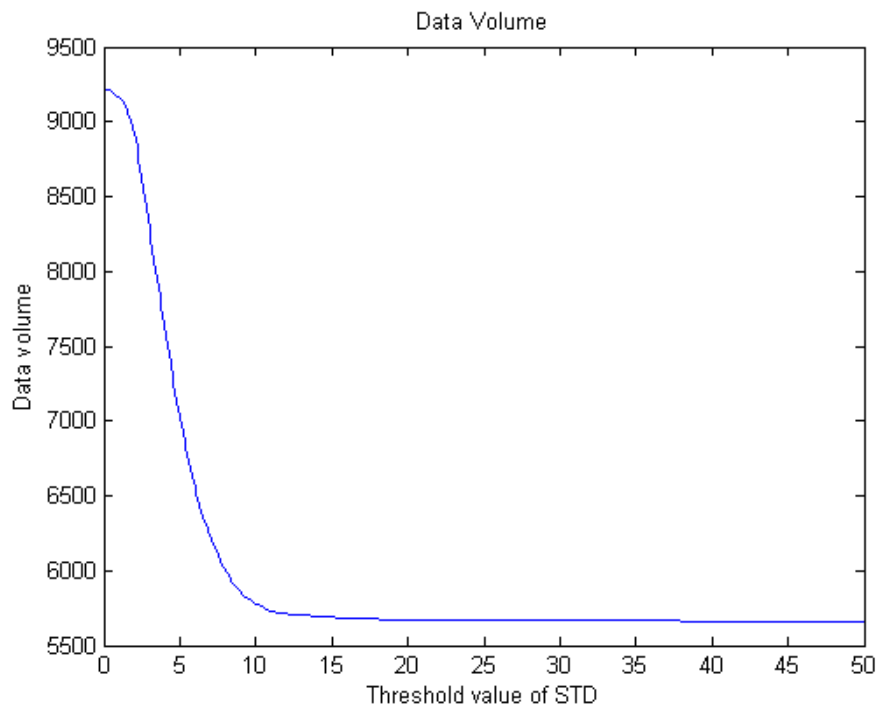


Figure 4.14: Data volume of adaptive probing

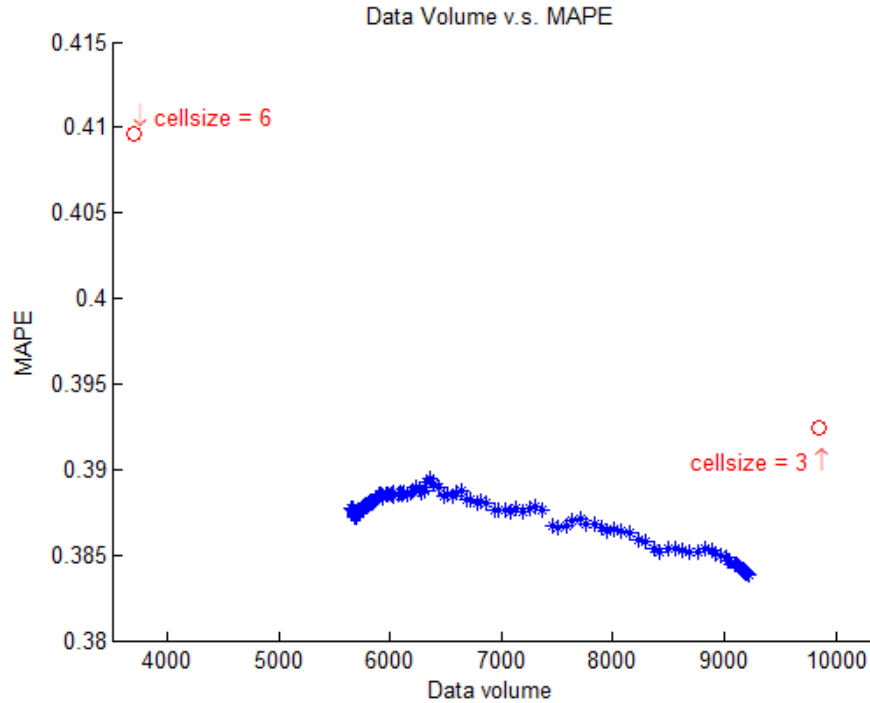


Figure 4.15: Data volume versus MAPE of adaptive probing

the result of prediction error and data volume changed with the threshold value of standard deviation, respectively. Figure 4.15 shows the relation between error and data volume from adaptive probing with different σ_{limit} value, and the result is also compared with non-adaptive probing in cell size of 6 and cell size of 3.

The result shows that adaptive probing performs better than non-adaptive probing under any σ_{limit} value. While adaptive probing is expected to be better than cell size of 6 because for the extra data collected, any adaptive probing can do better than non-adaptive probing using cell size of 3 with less data volume. Because the adaptive scheme does not only switch to a smaller cell size when σ is higher than a threshold value, it also allows the option of choosing between the prediction with lower standard deviation, or changing to a smaller cell size when the default cell size is not available. Therefore, even with $\sigma_{limit} = 0$ (always evaluate cell of 3 and 6 and choose the one with lower σ), or with very high σ_{limit} (use cell of 6, but allow cell of 3 if data not available with cell of 6), there is still improvement in prediction accuracy.

4.8 Conclusions

This chapter presented a stochastic Lagrangian LWR traffic flow model with the capability of estimating current and future traffic status with data collected by pairs of probing vehicle. The model and traffic state estimation can be updated with the observation data in real-time using dual UKF. The proposed model was validated by empirical highway traffic data, and the result showed that the stochastic model have an overall 20% improvement in estimating current traffic state comparing to the estimation from deterministic model. The predictive ability allows the model to predict traffic 3-second in the future with about 15% error, which can be used to compensate the latency of data transition and data process. The change of traffic phase to unexpected wide moving jam can be predicted by model parameters with a 6.76 sec lead time, so that the driver can be warned ahead of time. For the scenario that probing pairs are scarce, the result showed approximately 19% error due to the uncertainty in estimating the number of vehicles in a cell using loop detector data. Also, in this chapter, an adaptive control scheme was proposed by requesting additional data when the standard deviation of predication from stochastic model is high. The result showed that adaptive probing can improve information accuracy from non-adaptive probing with larger cell size. And by adaptively using prediction with higher confidence level (lower standard deviation) it can have better performance with lower data volume compared to non-adaptive probing with smaller cell size. Therefore, it is beneficial to have an adaptive probing strategy to utilize data efficiently.

CHAPTER V

Summary and Future Work

5.1 Dissertation Conclusion

This dissertation investigated macroscopic traffic flow model and probing strategy that can be used in an intelligent transportation system to predict traffic state in real-time utilizing traffic data collected by probe vehicles. In Chapter III Newtonian relaxation method was used to incorporate probing data into the LWR model in Eulerian coordinates for traffic status estimation. An optimization scheme of probe vehicle deployment was presented to reveal the trade-off between the quality of traffic flow estimation and operation cost. Synthetic data was used to test the model with numerical result, and Genetic algorithm was used to solve the optimization problem. The result showed that, optimal deployment of probe vehicle can reduce probing cost and estimation error by efficient usage of probe vehicles. By optimizing probing cost and prediction error, it is possible to reduce the operation cost by 40% with only 5% increase in error comparing to the optimization for prediction error only. So it is possible to decrease probing data for congested traffic with negligible degradation on the quality of traffic status estimation, and the probing strategy should be adaptive with traffic condition. In Chapter IV, the LWR model was then converted into Lagrangian coordinates with a forcing function to form a stochastic Lagrangian macroscopic traffic flow model. Unscented Kalman filter was used to update the prediction of model

parameters and traffic state in real-time. The proposed probing method tracks vehicles in pairs and utilizes loop detector data for additional information as needed. The model was validated with two sets of empirical data to demonstrate its capability of providing short-term prediction and using model parameter as a detector of traffic jam. The stochastic model had an overall 20 % improvement in estimating current traffic state comparing to the estimation from deterministic model, and 3-second prediction error was about 15%. The model parameter α can be used to detect jam with an average lead time of 6.76 sec. For the scenario that probing pairs are scarce, the result showed approximately 19% error due to the uncertainty in estimating the number of vehicles in a cell using loop detector data. Also, a scheme of adaptive probing was presented to demonstrate that it is possible to adjust probing strategy based on the variance output of the stochastic model. The experimental result showed that by adaptively using prediction with higher confidence level (lower standard deviation), it can have better performance with lower data volume compared to non-adaptive probing with higher data volume.

5.2 Contribution

The major contributions of this work are summarized as follows:

1. This dissertation proposed a stochastic Lagrangian traffic flow model that allows the usage of probe vehicle data, and a combination of probing and loop detector data. A unique way of probing vehicles in pairs was used for the Lagrangian model to collect average spacing between vehicles. While the assimilation of probing data with Eulerian traffic flow model is also feasible, this allows the choice between the Eulerian and the Lagrangian traffic flow model depending on the usage of traffic information and the point of view. Traffic management agency may prefer to use location as the coordinate to know where to imple-

ment traffic control strategy to relieve congestion. On the other hand, traffic information follow a platoon of vehicles as in the Lagrangian model is easier to distribute to the drivers inside or near the platoon.

2. This dissertation identified the potential of using short-term prediction and model parameter to detect wide moving jam phase in advance. This innovative way of detection allows individual driver to be alert before entering a traffic jam, so that the vehicle may be prepared for the stop-and-go traffic, or even reroute to avoid it. This information may not only benefit drivers in the predicted cell, but may also be used to notified other drivers in the entire traffic network. This detection method is different from other previous models that track existed traffic jam and require the initial identification of traffic phases using the comprehensive information from the transportation network.
3. This dissertation demonstrated the first investigation of probing strategy. The attempt of optimal probe vehicle deployment reveals the possibility for traffic management agency to optimally allocate probing vehicles into the traffic system for data collection. Furthermore, using the variance of prediction from stochastic model is an unique method to allow adaptive probing by adjusting the size of probing vehicle platoon. The proposed adaptive probing scheme is simple but effective in improving prediction accuracy and reducing the cost of data collection.

5.3 Future Work

While this dissertation provides a way to help with the traffic congestion problem, further investigation and other application can be explored in the future. Several potential topics for future research are described as below:

1. Investigation of performance bounds

The method proposed in this dissertation was validated by showing improved performance using simulated and experimental data. It is also possible to further investigate the performance bounds in theory or using simulations to understand the limitation of the model. This may not only provide an insight of the guaranteed information quality providing by the propose method, but may also reveal the potential of future improvement of the model.

2. Optimal sampling method for adaptive probing

In this dissertation, adaptive probing was shown to be a better probing method than fixed cell size probing, even when the proposed adaptive probing scheme is very simple. Further improvement in information quality and data volume reduction may be done by introducing optimization method for the sampling process of probing vehicle. Instead of simply adjusting the cell size of probing between two levels, optimization would allow a more sophisticated and robust method to decide how to sample the vehicles in the traffic. This may lead to a better efficiency in data utilization.

3. Traffic information distribution

While this dissertation focused on consolidating data collection, assimilation, and converting data into useful traffic information, traffic information distribution strategy can be the next ingredient to be added into the intelligent transportation system. Different market penetration rate of traffic information and the reliability of provided information may influence the benefit of using traffic information. Future investigation can be done when the penetration rate of information is related to the penetration rate of data, or independently consider the information distribution problem. The dynamics can be complicated when probed vehicles are expected to receive traffic information in return, but drivers might over-react to the predicted congestion and shift the congestion

across the network, which may negatively affect the accuracy of the prediction.

4. Optimal operation of probing commercial vehicle

One application of the optimal probing deployment proposed in this dissertation is to construct a system that incorporate commercial vehicles as probing sources. Tracking and communication equipments are usually available on those vehicles with no privacy concerns, and the cost of operating the probing can be low when delivery requirement is satisfied at the same time. However, the availability of probing data may be constrained by the delivery requirement of the commercial vehicle. An optimization problem considering both information quality and operation requirement of the commercial vehicle could be an interested application of the technology developed by the research in this dissertation.

BIBLIOGRAPHY

BIBLIOGRAPHY

- Auld, J., M. Hope, H. Ley, V. Sokolov, B. Xu, and K. Zhang (2015), Polaris: Agent-based modeling framework development and implementation for integrated travel demand and network and operations simulations, *Transportation Research Part C: Emerging Technologies*.
- Aw, A., and M. Rascle (2000), Resurrection of "second order" models of traffic flow, *SIAM journal on applied mathematics*, 60(3), 916–938.
- Balakrishna, R., H. Koutsopoulos, M. Ben-Akiva, B. Fernandez Ruiz, and M. Mehta (2005), Simulation-Based Evaluation of Advanced Traveler Information Systems, *Transportation Research Record*, 1910(1), 90–98.
- Barth, M., and K. Boriboonsomsin (2009), Energy and emissions impacts of a freeway-based dynamic eco-driving system, *Transportation Research Part D: Transport and Environment*, 14(6), 400–410.
- Barth, M., E. Johnston, and R. Tadi (1996), Using gps technology to relate macroscopic and microscopic traffic parameters, *Transportation Research Record: Journal of the Transportation Research Board*, 1520(1), 89–96.
- Boel, R., and L. Mihaylova (2006), A compositional stochastic model for real time freeway traffic simulation, *Transportation Research Part B*, 40(4), 319–334.
- Breitenberger, S., B. Gruber, M. Neuherz, and R. Kates (2004), Traffic information potential and necessary penetration rates, *Traffic Engineering and Control*, 45, 396–401.
- Chu, K.-C., L. Yang, R. Saigal, and K. Saitou (2011), Validation of Stochastic Traffic Flow Model with Microscopic Traffic Simulation, in *2011 IEEE International Conference on Automation Science and Engineering*, pp. 672–677, IEEE.
- Chu, L., H. Liu, and W. Recker (2004), Using microscopic simulation to evaluate potential intelligent transportation system strategies under nonrecurrent congestion, *Transportation Research Record: Journal of the Transportation Research Board*, (1886), 76–84.
- Courant, R., and K. O. Friedrichs (1999), *Supersonic flow and shock waves*, vol. 21, Springer Science & Business Media.

- Daganzo, C. F. (1994), The cell transmission model: A dynamic representation of highway traffic consistent with the hydrodynamic theory, *28*(4), 269–287.
- Daganzo, C. F. (1995), Requiem for second-order fluid approximations of traffic flow.
- Daganzo, C. F. (2005), A variational formulation of kinematic waves: basic theory and complex boundary conditions, *Transportation Research Part B: Methodological*, *39*(2), 187–196.
- Deb, K. (2001), Multi-objective optimization, *Multi-objective optimization using evolutionary algorithms*, pp. 13–46.
- FHWA (2004), Status of the Nation’s Highways, Bridges, and Transit: 2004 Conditions and Performance.
- Gipps, P. G. (1986), A model for the structure of lane-changing decisions, *Transportation Research Part B: Methodological*, *20*(5), 403–414.
- Godunov, S. K. (1959), A difference method for numerical calculation of discontinuous solutions of the equations of hydrodynamics, *Matematicheskii Sbornik*, *89*(3), 271–306.
- Goldbach, M., A. Eidmann, and A. Kittel (2000), Simulation of multilane freeway traffic with detailed rules deduced from microscopic driving behavior, *Physical Review E*, *61*(2), 1239.
- Greenberg, H. (1959), An analysis of traffic flow, *Operations Research*, *7*(1), 79–85.
- Greenshields, B., J. Bibbins, W. Channing, and H. Miller (1935), A study of traffic capacity, in *Highway Research Board Proceedings*.
- Hegyi, A., D. Girimonte, R. Babuska, and B. D. Schutter (2006), A comparison of filter configurations for freeway traffic state estimation, in *Intelligent Transportation Systems Conference, 2006. ITSC '06. IEEE*, pp. 1029–1034.
- HERE (2016), Here predictive traffic.
- Herrera, J., and A. Bayen (2010), Incorporation of Lagrangian measurements in freeway traffic state estimation, *Transportation Research Part B: Methodological*, *44*(4), 460–481.
- Herrera, J. C., D. B. Work, R. Herring, X. Ban, Q. Jacobson, and A. M. Bayen (2010), Evaluation of traffic data obtained via GPS-enabled mobile phones: The Mobile Century field experiment, *Transportation Research Part C: Emerging Technologies*, *18*(4), 568–583.
- Hodas, N. O., and A. Jagota (2003), Microscopic modeling of multi-lane highway traffic flow, *American Journal of Physics*, *71*(12), 1247.

- Jones, D. R., M. Schonlau, and W. J. Welch (1998), Efficient global optimization of expensive black-box functions, *Journal of Global optimization*, 13(4), 455–492.
- Julier, S., and J. Uhlmann (2004), Unscented Filtering and Nonlinear Estimation, *Proceedings of the IEEE*, 92(3), 401–422.
- Kalman, R. E., et al. (1960), A new approach to linear filtering and prediction problems, *Journal of basic Engineering*, 82(1), 35–45.
- Kang, N., B. Kim, and H. Kim (2005), Optimal route planning algorithm based on real traffic network, *SAE transactions*, 114(7).
- Kerner, B. S. (2009), *Introduction to Modern Traffic Flow Theory and Control*, Springer Berlin Heidelberg, Berlin, Heidelberg.
- Kerner, B. S., H. Rehborn, M. Aleksic, and A. Haug (2004a), Recognition and tracking of spatialtemporal congested traffic patterns on freeways, *Transportation Research Part C: Emerging Technologies*, 12(5), 369–400.
- Kerner, B. S., H. Rehborn, M. Aleksic, and A. Haug (2004b), Recognition and tracking of spatialtemporal congested traffic patterns on freeways, *Transportation Research Part C: Emerging Technologies*, 12(5), 369 – 400.
- Kerner, B. S., H. Rehborn, R. P. Schäfer, S. L. Klenov, J. Palmer, S. Lorkowski, and N. Witte (2013), Traffic dynamics in empirical probe vehicle data studied with three-phase theory: Spatiotemporal reconstruction of traffic phases and generation of jam warning messages, *Physica A: Statistical Mechanics and its Applications*, 392(1), 221–251.
- Kurihara, S., H. Tamaki, M. Numao, J. Yano, K. Kagawa, and T. Morita (2009), Traffic congestion forecasting based on pheromone communication model for intelligent transport systems, *Evolutionary Computation, 2009. CEC '09. IEEE Congress on*.
- Lebacque, J.-P. (1996), The godunov scheme and what it means for first order traffic flow models, in *International symposium on transportation and traffic theory*, pp. 647–677.
- Leclercq, L., J. A. Laval, and E. Chevallier (2007), The lagrangian coordinates and what it means for first order traffic flow models, in *Transportation and Traffic Theory 2007. Papers Selected for Presentation at ISTTT17*.
- Li, J., Q.-Y. Chen, H. Wang, and D. Ni (2012), Analysis of LWR model with fundamental diagram subject to uncertainties, *Transportmetrica*, 8(6), 387–405.
- Lighthill, M., and G. Whitham (1955), On kinematic waves. II. A theory of traffic flow on long crowded roads, *Proceedings of the Royal Society of London. Series A, Mathematical and Physical Sciences*, pp. 317–345.

- MATLAB (2012), *version 7.14.0 (R2012a)*, The MathWorks Inc., Natick, Massachusetts.
- Mazaré, P., and O. Tossavainen (2012), Trade-offs between inductive loops and GPS probe vehicles for travel time estimation: A Mobile Century case study, *Transportation Research Board 91st Annual Meeting*, 61801(217).
- Mihaylova, L., R. Boel, and A. Hegyi (2007), Freeway traffic estimation within particle filtering framework, *Automatica*, 43(2), 290 – 300.
- MIT Intelligent Transportation Systems Program (2010), Mitsimlab, <http://its.mit.edu/software>.
- Newell, G. (1993), A simplified theory of kinematic waves in highway traffic, part III: Multi-destination flows, 27(4), 305–313.
- Papageorgiou, M., J.-M. Blosseville, and H. Hadj-Salem (1990), Modelling and real-time control of traffic flow on the southern part of boulevard peripherique in paris: Part i: Modelling, *Transportation Research Part A: General*, 24(5), 345–359.
- Payne, H. J. (1971), Models of freeway traffic and control., *Mathematical models of public systems*.
- Pipes, L. A. (1953), An operational analysis of traffic dynamics, *Journal of applied physics*, 24(3), 274–281.
- PTV Planung Transport Verkehr AG (2011), Ptv visum, <http://www.vissim.de>.
- Quadstone Paramics Ltd (2011), Quadstone paramics, <http://www.paramics-online.com/>.
- Rehborn, H., S. L. Klenov, and J. Palmer (2011), An empirical study of common traffic congestion features based on traffic data measured in the USA, the UK, and Germany, *Physica A: Statistical Mechanics and its Applications*, 390(23-24), 4466–4485.
- Rehborn, H., B. Kerner, and R. Schäfer (2012), Traffic Jam Warning Messages from Measured Vehicle Data with the Use of Three-Phase Traffic Theory, *Advanced Microsystems for ...*, pp. 241–250.
- Richards, P. I. (1956), Shock wWaves on the Highway, *Operations Research*, 4, 42–51.
- Saigal, R., L. Yang, C. Chu, and Y. Wan (2011), Stochastic model for traffic flow prediction and its validation, *Transportation Research Board 90th Annual Meeting*.
- Schrank, D., B. Eisele, T. Lomax, and J. Bak (2015), Urban mobility scorecard, *Tech. rep.*, Technical Report August, Texas A&M Transportation Institute and INRIX, Inc.
- TSS-Transport Simulation Systems (2010), Aimsun, <http://www.aimsun.com>.

- Underwood, R. (1961), Speed, volume, and density relationships: Quality and theory of traffic flow, *Speed, Volume, and Density Relationships: Quality and Theory of Traffic Flow*, pp. 141–188, cited By (since 1996) 25.
- US Department of Transportation (2006), Next Generation Simulation (NGSIM), <http://ops.fhwa.dot.gov/trafficanalysistools/ngsim.htm>, accessed on June 3, 2013.
- Van Wageningen-Kessels, F., Y. Yuan, S. P. Hoogendoorn, H. Van Lint, and K. Vuik (2013), Discontinuities in the Lagrangian formulation of the kinematic wave model, *Transportation Research Part C: Emerging Technologies*, 34, 148–161.
- Walsh, J. (1986), An introduction to stochastic partial differential equations, *Lecture Notes in Math*, 1180(265), 439.
- Wang, Y., and M. Papageorgiou (2005), Real-time freeway traffic state estimation based on extended Kalman filter: a general approach, *Transportation Research Part B: Methodological*, 39(2), 141–167.
- Wang, Y., M. Papageorgiou, and A. Messmer (2007), Real-Time Freeway Traffic State Estimation Based on Extended Kalman Filter: A Case Study, *Transportation Science*.
- Whitham, G. (1974), Linear and nonlinear waves, *John Wiley & Sons, New York*.
- Work, D. B., S. Blandin, O. P. Tossavainen, B. Piccoli, and A. M. Bayen (2010), A Traffic Model for Velocity Data Assimilation, *Applied Mathematics Research eXpress*, 2010(1), 1–35.
- Yang, L. (2012), Stochastic traffic flow modeling and optimal congestion pricing, Ph.D. thesis, The University of Michigan.
- Yuan, Y., J. W. C. van Lint, R. E. Wilson, F. van Wageningen-Kessels, and S. P. Hoogendoorn (2012), Real-Time Lagrangian Traffic State Estimator for Freeways, *IEEE Transactions on Intelligent Transportation Systems*, 13(1), 59–70.
- Zhang, H. M. (2002), A non-equilibrium traffic model devoid of gas-like behavior, *Transportation Research Part B: Methodological*, 36(3), 275–290.